MOLECULAR BASIS OF PRION PATHOGENESIS AND DEVELOPMENT OF A NOVEL THERAPEUTIC STRATEGY

Committee:

Claudio Soto, PhD. (Supervisor)

Claudio Hetz, PhD.

Jose R. Perez-Polo, PhD.

Giulio Taglialatela, PhD.

Jose M. Barral, PhD.

Dean, Graduate School

MOLECULAR BASIS OF PRION PATHOGENESIS AND DEVELOPMENT OF A NOVEL THERAPEUTIC STRATEGY

by

Abhisek Mukherjee, B.Sc, M.Sc

Dissertation

Presented to the Faculty of the Graduate School of

The University of Texas Medical Branch

in Partial Fulfillment

of the Requirements

for the Degree of

DOCTOR OF PHILOSOPHY

The University of Texas Medical Branch

March, 2012

Dedication

I dedicate my thesis to the families who are desperately seeking for a cure of prion disease to save their near and dear ones.

Acknowledgements

While my dissertation bears my name alone, this work would not have been possible without the support of many individuals in the United States and in India. I would not be the researcher I am today without their inspiration and mentorship. With deep gratitude I would like to acknowledge their contribution.

First I would like to thank the Graduate School of Biomedical Sciences of UTMB for accepting me in the doctoral degree program and providing me the opportunity to work with such an excellent academic community. I convey my deep gratitude to Dr. Dorian H. Coppenhaver for supporting me from day one in GSBS and Ms. Jessica E. Linton for her patience to reply all my queries from the day before I even joined GSBS. I would also like to convey a special thanks to Dr. Cary W. Cooper for supporting me while I was going through an extremely difficult period of my life.

I would like to thank Dr. Lillian Chan for guiding me in the initial days after I joined the Biochemistry and Molecular Biology graduate program and Ms. Debora M. Botting who always came out of her way to help me whenever I needed it.

My deep gratitude to the members of dissertation committee Dr. Jose R. Perez-Polo, Dr. Jose M. Barral, Dr. Giulio Taglialatela and Dr. Claudio Hetz for their help support ,critical analysis and very important suggestions throughout my thesis.

I would like to thank Dr. Marcie Glicksman, Dr. Greg Cuny and Dr. Kathleen Syeb from Harvard Neuro Discovery Center at Cambridge, MA. for providing in depth understanding and hands on training on high throughput screening of small molecule

inhibitors. This knowledge helped me a lot to translate my dissertation research in to a drug discovery project.

I would like thank my friends Mr. Aditya Hindupur , Mr. Rohit Jangra, Mr Aditya Joshi, Dr. Truptesh Kothari, Mr. Marcelo Barria, Ms. Dennisse Gonzalez, Ms. Diego Morales, Mr. Rodrigo Diaz and Mr. Rodrigo Morales who made my stay in UTMB memorable and supported me in the days of hardship.

I would like thank my father Dr. Gautam Mukherjee and my mother Mrs. Chandra Mukherjee for their continuous encouragement, love and support which helped me to travel a long way to come to this point where I am finally writing my thesis. I would also like to thank my brother Mr. Shaon Mukherjee not only for his love and respect but also for his belief in me. I am thankful to my mother-in-law Mrs. Ira Chatterjee and father-in-law Mr. Gurubandhu Chatterjee for their help and support as they took care of everything so that I could solely concentrate in my research while preparing my dissertation.

Without my wife Priyanka, this thesis was almost impossible. Starting from editing important scientific presentations to proof reading the draft of the thesis she was the one I solely depended on. She tried her level best to support me even while going through extreme health conditions. Her entertaining daily life stories brought me smile even at the end of a most disheartening day of failure. I am fortunate to have her as wife and I would like to convey my deepest thanks to her.

Finally, I would like to thank the person who made this thesis possible, my mentor Dr. Claudio. Soto. I would like to thank him for accepting me in his laboratory

and providing me the opportunity to work with such a diverse group of people in a joyful environment. I am still learning analytical skills and ability to accept criticism from him. I would like to thank him for providing the time from his busy schedule for the bi-weekly meeting sessions throughout my dissertation. Those discussions were really beneficial for me not only to develop my dissertation research but also to develop myself as scientific researcher. His strong optimism helped me to forget the pain of repeated failures and finally reach the goal. He is not only a mentor but became an outstanding friend in the soccer fields or in difficult times of life. He taught me how to think. He encouraged me to think out of the box. And finally he supported me to develop my own thoughts in to a successful project. I would like to convey my deepest gratitude to Dr. Claudio Soto.

MOLECULAR BASIS OF PRION PATHOGENESIS AND DEVELOPMENT OF A NOVEL THERAPEUTIC STRATEGY

Publication No._____

Abhisek Mukherjee, PhD

The University of Texas Medical Branch, 2012

Supervisor: Claudio Soto

Prion diseases are fatal neurodegenerative disorders characterized by a long pre-symptomatic phase followed by rapid and progressive clinical phase. Although rare in humans, the unconventional infectious nature of the disease raises the potential for an epidemic. Unfortunately, no treatment is currently available. The hallmark event in prion diseases is the accumulation of a misfolded and infectious form of the prion protein (PrP^{Sc}). Previous reports have shown that PrP^{Sc} induces endoplasmic reticulum stress and changes in calcium homeostasis in the brain of affected individuals. My research shows that the calcium-dependent phosphatase Calcineurin (CaN) is hyperactivated both *in vitro* and *in vivo* as a result of PrP^{Sc} formation. CaN activation mediates prion-induced neurodegeneration, suggesting that inhibition of this phosphatase could be a target for therapy. To test this hypothesis, prion-infected wild type mice were treated intra-peritoneally with the CaN inhibitor FK506 at the clinical phase of the disease. Treated animals exhibited reduced severity of the clinical abnormalities and increased survival

time compared to vehicle treated controls. Treatment also led to a significant increase in the brain levels of the CaN downstream targets pCREB and pBAD, which paralleled the decrease of CaN activity. Importantly, I observed a lower degree of neurodegeneration in animals treated with the drug as revealed by a higher number of neurons and a lower quantity of degenerating nerve cells. These changes were not dependent on PrP^{Sc} formation, since the protein accumulated in the brain to the same levels as in the untreated mice. My findings contribute to an understanding of the mechanism of neurodegeneration in prion diseases and more importantly may provide a novel strategy for therapy that is beneficial at the clinical phase of the disease.

Table of Contents

Chapter 1: Introduction ***1***

1.1 Prion Diseases 1

1.2 Prion Protein 2

1.2.1 Structure 2

1.2.2 Proposed Function 3

1.3 ER Stress in Prion Disease 5

1.4 Calcineurin Biology 8

1.5 Calcineurin in Neural Homeostasis 10

1.6 Prion Disease Treatment 11

1.7 Hypothesis 12

Chapter 2: Materials & Methods ***13***

2.1 Ethics Statement 13

2.2 FK506 Preparation 13

2.3 CaN Activity Assay 14

2.4 Purification of PrP^{C} and PrP^{Sc} 14

2.5 Cell Toxicity Studies (MTT & LDH assay) 15

2.6 Determination of Cytoplasmic Calcium 16

2.7 Animal Model of Prion Disease 16

2.8 Animal Treatment 17

2.9 Animal Behavioral Tests 17

2.10 PrP^{Sc} Detection Assay 17

2.11 Detection of pCREB & pBAD 18

2.12 Postmortem Neuropathological Analysis 19

2.13 Enzyme Assay 21

2.14 Enzyme Inhibition Assay 22

2.15 Miniaturization of the Enzyme Assay 22

2.16 Statistical Analysis 23

Chapter 3: PrP^{Sc}-Induced Toxicity is Mediated by CaN Activation 24

Chapter 4: Optimization of CaN Activity Inhibits Prion Disease Progression in Mouse Model 29

4.1 Inhibition of CaN Activity Decreases Disease Severity and Increases Animal Survival 30

4.2 FK506 Treatment Does Not Alter PrP^{Sc} Accumulation but Increase pCREB AnD pBAD 33

4.3 Astrogliosis and Microgliosis Were Not Altered By CaN Inhibition 37

4.4 Reduction of Neurodegeneration By

CaN Inhibition In Prion Affected Mice 39

Chapter 5: Development Of A Robust Assay To Screen Novel Inhibitor Against CaN ***42***

5.1 Characterization of CaN Enzyme Activity 42

5.2 Technical Standardizations 45

5.3 Miniaturization of the Assay 47

5.4 Automation of the Assay 51

Chapter 6: Conclusion ***53***

Appendix ***58***

Glossary ***61***

References ***64***

Vita ***73***

List of Figures

Figure 3.1:	***PrP^{Sc} induces CaN activation.***	***25***
Figure 3.2:	***PrP^{Sc} induced cell death is rescued by CaN inbition.***	***27***
Figure 3.3:	***Over-activation of CaN at the clinical phase of prion disease mouse model.***	***28***
Figure 4.1:	***Inhibition of CaN reduces disease progression.***	***31***
Figure 4.2:	***Increase in survival of prion infected animals by treatment with CaN inhibitor.***	***33***
Figure 4.3:	***Effect of FK506 treatment on PrP^{Sc} formation and CaN activity.***	***34***
Figure 4.4:	***Recovery of pCREB and pBAD level by optimization of CaN activity.***	***36***
Figure 4.5:	***Unaltered astrogliocis and microgliocis after FK506 treatment.***	***38***
Figure 4.6:	***Treatment with FK506 decreases prion-induced neuronal loss.***	***40***
Figure 4.7:	***CaN inhibitor reduces neurodegeneration in prion infected animals.***	***41***
Figure 5.1:	***Characterization of Enzyme Activity.***	***43***
Figure 5.2:	***Technical standardizations.***	***45***
Figure 5.3:	***Miniaturization of the assay.***	***48***
Figure 5.4:	***Validation of the assay.***	***50***

CHAPTER 1

INTRODUCTION [1]

1.1 PRION DISEASES:

Prion diseases or transmissible spongiform encephalopathies (TSEs) are lethal, infectious disorders affecting the mammalian nervous system. The family of TSEs includes scrapie in sheep, bovine spongiform encephalopathy (BSE) or ‘‘mad cow disease’’ in cattle, and several human neuropathies: Creutzfeld–Jacob disease (CJD), fatal familial insomnia (FFI), Gertsmann–Straussler–Scheinker (GSS) syndrome, and kuru. TSEs are relatively rare in human. However the recent appearance of a new form of CJD, termed[1] variant CJD (vCJD), and the fact that the pathogen is biochemically linked to a BSE agent [1] has raised concerns about a possible outbreak of a large epidemic in the human population. While around 10-15% of all the human cases, including all GSS and FFI, have been reported to be inherited in an autosomic dominant manner, most of the cases (85%) [2] are sporadic where the cause that triggers the disease remains to be explained. The intriguing feature that distinguishes TSEs from other neurodegenerative

[1] A significant amount of this paragraph has been previously published in the following articles.
(Reproduced with permission, see appendix)

Mukherjee, A., Soto.C (2009) ER Stress response in Prion Diseases. ***Bentham e Books.*** **eISBN:** 978-1-60805-013-0.

Mukherjee,A., Soto,C. Role of Calcineurin in Neurodegeneration Produced by Misfolded Proteins and Endoplasmic Reticulum Stress. ***Current opinion in Cell Biology***. 2011 Apr;23(2):223-30

diseases associated to protein misfolding is the infectious nature of the disease. Surgical supplies, cornea transplant or human growth hormone from affected individuals have been described to transmit the disease to normal individual [3]. Recent report of transmission of vCJD by blood transfusion [4] set up a red alert throughout European blood banks.

1.2 PRION PROTEIN:

The hallmark neuropathological features of TSEs are the spongiform degeneration of the brain, extensive synaptic dysfunction, neuronal loss, astrogliosis, and cerebral accumulation of PrP^{Sc} aggregates [5]. Although the relationship between different brain abnormalities in TSE is not clear the conversion of the cellular form of prion protein (PrP^{C}) into an abnormally folded form (PrP^{Sc}) and accumulation of PrP^{Sc} in the nervous system has been shown to be the central event in TSE pathogenesis.

1.2.1 Structure: Prion protein is a type 1 membrane protein expressed in wide variety of tissues, but expression in brain is much higher. In mammals, the sequence of PrP is highly conserved. Human prion precursor protein consists of 253 amino acids. Irrespective of the species, it has an N-terminal signal sequence that directs it towards the endoplasmic reticulum (ER) followed by a less structured domain (residue 23-134). This domain consists of several octapeptide repeat (OR) flanked between two positively charged CC1 and CC2 (residue 23-27 and 95-110 respectively).The N-terminal is linked to C-terminal by a hydrophobic stretch called HC region (residue 111-134) [6]. The C–terminal is globular in structure and contains signal domain that determines its

association to lipid rafts through glycophosphatidyl inositol (GPI) anchoring [7-9]. PrP is glycosylated in two (Asparagin-181 and Asparagin-197) sites during ER-Golgi trafficking. The protein is found as a mixture of mono-, di- and un-glycosyalted forms. The fact that PrP^{C} glycosylation is conserved in mammals suggests an important role of the sugar moieties [7]. Prion protein also has a disulfide bridge which is very important for its structure. PrP is mostly attached to the exterior leaflet of the cell membrane [10], but it can also retro-translocate from ER to cytoplasm resulting in cytosolic PrP (CyPrP) [11]. The mature human prion protein consists of 209 amino acids. The length varies slightly in different species.

1.2.2 Proposed Function: Although several putative activities have been described for PrP^{C}, its physiological function is still poorly understood [12;13]. One of the major proposed functions was Cu^{2+} binding and contributing towards the redox balance of the cell. However the observation that the PrP null neural cells accumulate Cu^{2+} is severely questioned later [14;15]. PrP^{C} null neural cells have also been suggested to be more prone to apoptosis under serum deprivation. Further studies raveling that PrP^{C} is able to inhibit apoptosis produced by the over expression of Bax or TNF-α suggested PrP^{C} to be involved in an anti apoptotic signaling [16;17]. Therefore loss of function of PrP^{C} due to conversion in to PrP^{Sc} may be speculated to contribute in the prion disease pathogenesis. Severe neuronal damage produced in the hippocampus by abolishing PrPC function using anti-PrP^{C} antibodies strongly supported this hypothesis [18]. However recent demonstration of efficient therapeutic intervention against prion disease by anti-PrP antibody strongly questions this theory [19]. Finally, the fact that PrP null and conditional

knockout animals do not show any gross phenotype suggests that all these proposed functions may not be critical for viability [20-23]. Therefore, the gain of toxic function, by the conversion of cellular prion protein in to a partially protease-resistant, detergent insoluble form (PrP^{Sc}) became the widely accepted theory to explain the pathogenesis in TSEs. However it is difficult to imagine that the sole important function of a protein which is so conserved among the mammals is to confer susceptibility to PrP^{Sc}. Therefore further research should be done to investigate the function of PrP^{C}.

As the name suggests, TSEs belongs to a new class of unprecedented transmissible and the infectious agents whose nature of pathogenesis is not yet fully known. Compelling evidences suggest that PrP^{Sc} is the sole component of the infectious agent [24]. It has been proposed that infectious prion particles interact and convert the host PrP^{C} in to a protease resistant detergent insoluble toxic form by inducing a conformational shift. Interestingly there is no change in primary structure involved in this process of conversion. A conformational change from high level α-helical content of PrP^{C} to high β-sheet induce the formation of PrP^{Sc} [24]. Although mechanism of this conformational change is not clear yet, binding of PrP^{C} with the abnormally folded protein followed by oligomerization and acquisition of partial protease resistance has been shown in cell free conversion system [25]. Irrespective of how the misfolding occurs, it plays a paramount role in mediating neurodegeneration and transmitting infectivity. However, despite massive investigation, little is known about cellular factors modulating the conversion and how the generation of PrP^{Sc} leads to brain damage.

1.3 ER STRESS IN PRION DISEASE:

Previous work from my lab has shown that purified PrP^{Sc} from scrapie-infected brains is able to induce cell death in primary neuron cultures. The study demonstrated that the cellular pathway controlling the induction of apoptosis involves stress of the endoplasmic reticulum (ER). ER is an important organelle for the synthesis, folding, and transport of nascent proteins. Almost all secreted and membrane proteins, which are around 1/3 of the total cellular proteins, including PrP^{C}, attain their folded conformation in the ER. The correct folding of a protein inside the ER involves proper post-translational modification such as glycosylation and disulfide bond formation. Conditions such as a reducing environment, viral infection, glucose starvation, inhibition of glycosylation, perturbation of Ca^{2+} homeostasis, inhibition of proteosome disturbs the integrity of the ER, which finally results in a burden of misfolded proteins [26;27]. Accumulation of misfolded proteins is sensed by the ER and it signals the nucleus to induce the genes required to combat against these misfolded proteins. This intracellular signaling event in response to ER stress is called Unfolded Protein Response (UPR). UPR consist of activation of three different mechanisms: (i) translational attenuation to decrease load of misfolded proteins in the ER. (ii) Transcriptional activation of different ER resident chaperones, including BiP/(glucose regulated protein) grp78, Protein Disulfide Isomerase, grp94 and grp58, to combat against misfolding. Up-regulation of UPR responsive chaperones, was observed in the cortex of patients affected with variant and sporadic Creutzfeldt-Jacob disease, in mice infected with scrapie prions and in neuroblastoma cells treated with brain-derived PrP^{Sc}. Moreover, the overexpression of the

disulfide isomerase grp58 was shown to be an early event in prion pathogenesis, closely following PrP^{Sc} formation. The interaction between PrP and this chaperone modulates the neurotoxic activity of PrP^{Sc}. (iii) Activation of ER associated degradation (ERAD) of proteins by directing them back to the cytosol for 26S proteasome mediated clearance. Wild type and disease associated mutant of prion protein has been shown to retrotranslocate to cytosol using ERAD. Furthermore accumulation of this cytosolic PrP has been shown to form PrP^{Sc} like structure leading to neural toxicity both in cell and animal model [28]. Recent demonstration of a Pre-Emptive Quality Control (pQC) pathway in presence of an acute ER stress provides one more way to direct ER bound proteins into proteasomic degradation in presence of an existing protein overload in the ER lumen [29;30]. It should be noted that pQC is mechanistically and spatially different from the ERAD pathway. While in ERAD the misfolded protein from ER is retro-translocated into the cytosol, the nascent ER bound protein is not able to enter the lumen of ER during activation of pQC. In general pQC works as a defensive mechanism protecting ER from protein overload. However in presence of a chronic ER stress contentious flow of PrP in to cytosol by pQC may lead to accumulation of toxic PrP.

The mechanisms described above alleviate cellular stress by either correcting the misfolding or clearing the misfolded proteins in a direct or indirect fashion [26;31]. This comprises the protective part of the ER stress response. However, in presence of long sustained stressing conditions or chronic production of misfolded proteins, the protective mechanisms are not enough to relieve the cells. In these conditions, ER stress lead to a

suicidal response when the cell is no more able to handle the burden of misfolded and unfunctional proteins.

Disruption of calcium homeostasis in the cell is probably the most adverse and immediate effect caused by ER stress produced by chronic accumulation of misfolded proteins[27;31]. Alterations in calcium homeostasis have also been reported in different neurodegenerative disorders associated with accumulation of misfolded aggregates, including AD, PD, HD, ALS and TSE [27;31]. Compared to other types of cells, the effect becomes even more deleterious to neurons, because of the significant role of calcium waves in neuronal activity. Ca^{2+} plays an important role as a second messenger in different cellular signaling pathways, where the final outcome is controlled by cellular calcium concentration. For this reason, maintaining a specific Ca^{2+} concentration in the cytoplasm is critical for normal neuronal biology. Cell utilizes different Ca^{2+} channels and ATP driven Ca^{2+} pumps to maintain a Ca^{2+} gradient and to stabilize the calcium homeostasis inside the cytoplasm [32]. ER functions as an intra-cellular Ca^{2+} storage. Ca^{2+} uptake into the ER from cytoplasm is guided by sarcoplasmic/ER Ca^{2+} ATPase (SERCA) and released via inositol 1,4,5-triphosphate receptor (IP_3R) or Raynodine receptor (RyR)[33]. Several studies have suggested increase of cytoplasmic Ca^{2+} due to ER stress in presence of misfolded proteins in various neurodegenerative diseases [27]. Previous work from our lab and others has reported the release of calcium from the ER to the cytoplasm when cells are exposed to misfolded prion protein. Indeed, Ca^{2+} release appears to be one of the first adverse effects after prion infection in cells. Recent

evidences strongly suggest that at least a major source of elevated Ca2+ in the cytoplasm of prion infected cells is leakage from the ER [34].

Among the consequences of protein misfolding mediated through ER stress and alterations in calcium homeostasis are changes on the activity of various kinases and a specific phosphatase in the neurons called calcineurin. The fact that (CaN) is the only Ca^{2+} dependent phosphatase present in the neuron draws an immediate attention.

1.4 CALCINEURIN BIOLOGY:

CaN is a Ca2+/Calmodulin dependent serine/threonine phosphatase highly abundant in mammalian brain tissue [35]. Insensitivity of CaN towards heat stable inhibitor proteins and its ability to preferentially dephosphorylate the α-subunit of phosphorylase kinase distinguish CaN from phosphatase type 1 and classify it under phosphatase type 2 (PP2). Ca2+ dependency of CaN sub-classify this enzyme under phosphatase type 2B (PP2B) and distinguish it from spontaneously active PP2A or Mg2+-dependent PP2[36-38]. Since the identification of CaN in late 1970s and ground-breaking discovery that it is the target of immunosuppressive drugs cyclosporine A and FK506 [39-41], extensive studies have been done to determine the structure and function of CaN. CaN is a heterodimer composed of a 60 KDa catalytic subunit (calcineurin A; CnA) and an 18 KDa regulatory subunit (calcineurin B; CnB) [38;42].Although the amino acid sequence of the catalytic domain is homologous to other serine/threonine protein phosphatases, the presence of three other regulatory domains in the carboxy-terminal of the subunit A distinguish CaN from others [38]. These domains are the CnB binding domain, the calmodulin-binding domain and the auto-inhibitory domain (CnAI)

that binds to the active site in the absence of Ca^{2+}/Calmodulin, inhibiting the enzyme activity. Ca2+/Calmodulin complex binds to subunit A with very high affinity followed by release of the auto-inhibitory domain from the active site, leading to enzymatic activation [43;44]. Kinetic studies revealed that there is roughly 15-times increase in the enzyme activity in presence of Ca^{2+}/Calmodulin complex [45]. CaN can be phosphorylated in the calmodulin-binding region. However, calmodulin can still bind and activate CaN in the phosphorylated state.

The mature CnB subunit is missing the initiator methionine, and the α-amino group of glycine at position 2 is modified by acylated myristric acid [42]. This post-translational modification is conserved throughout the evolution suggesting a crucial physiological role. However non-myristoylated CaN displays similar biological function [42]. Besides activation by calcium, CaN might be activated at least in two other ways involving proteolysis. Caspase-mediated cleavage of the CaN auto-inhibitory domain and the calmodulin-binding domain renders the enzyme constitutively active and insensitive to Ca^{2+}/Calmodulin [46]. However, due to the fact that activation of caspases is a downstream process during apoptosis, the biological significance of this cleavage is questionable. Another, seemingly more relevant, way of constitutive CaN activation is partial proteolysis by Ca^{2+}-dependent cysteine protease called calpain [47]. In vitro MALDI-TOF analysis has identified three different carboxy-terminal truncated forms of CaN after calpain cleavage corresponding to 45, 48 and 57 kDa fragments [47]. Among them the 45 kDa fragment does not contain either the calmodulin-binding domain or the auto-inhibitory domain leading to a Ca^{2+}/Calmodulin insensitive, constitutively active

enzyme [48]. Samples from human Alzheimer's brain showed the presence of the 57 kDa fragment, missing only the auto-inhibitory domain [49]. This fragment is still Ca^{2+}/Calmodulin sensitive. However, the truncation remarkably enhances the enzyme activity [49].

1.5 CALCINEURIN IN NEURAL HOMEOSTASIS:

CaN is found throughout the phylogenic tree and present in all mammalian tissues with high abundance in the cytosol, pre- and post-synaptic terminals in neurons [50]. The fact that CaN is the only Ca^{2+}-dependent phosphate present in neurons suggests that it might play a crucial role in maintenance of cellular homeostasis under Ca^{2+} oscillations. In fact, the putative role of CaN in neuronal activity has been studied extensively [50;51]. Ca^{2+} influx in the neuronal cytosol modulates activity of different sets of proteins to initiate the downstream signaling mechanism. Due to very high affinity (0.1-1nM) for Ca2+/CaM and co-localization with N-methyl-D-aspartate receptor, CaN activates promptly after cytoplasmic Ca^{2+} influx [44;52] . Upon activation, CaN contributes to inhibit further Ca^{2+} influx into the cytosol. CaN performs this task in multiple ways. It slows down the Ca2+ influx from plasma membrane by weakening voltage-gated Ca^{2+} channels as well as regulates Ca^{2+}-induced Ca^{2+} release from the ER by negatively controlling IP3 and RyR through dephosphorylation [53;54].

The importance of CaN is not restricted to the regulation of Ca^{2+} influx into the cytosol, but it has also been shown that CaN plays an important role in modulating gene expression. In neurons one of the major transcription factors working under the control of CaN is cAMP–response element binding protein (CREB) [42;52]. CREB is

phosphorylated by Ca2+-dependent and independent protein kinases and translocate into the nucleus followed by to induce gene expression. CREB-induced gene expression is required for different sets of proteins involved in neuronal growth and survival, including BDNF and its receptor tropomyosin related kinase B (trkB) [55;56;56-58]. However, chronically activated CaN has been shown to dephosphorylate and inactivate CREB, subsequently shutting down the CREB-dependent gene expression [59], leading to loss of synaptic plasticity [50;51;59]. Over-activated CaN is implicated in a reversible (operated by post-translational modifications) neuronal apoptotic pathway involving Bcl-2 family proteins [32]. Hyper-activation of CaN due to chronic increase of cytoplasmic Ca^{2+}, reduces the phosphorylation of pro-apoptic BAD [60;61], which in the normal phosphorylated state is associated with scaffolding protein 14-3-3. However, dephosphorylated BAD disassociate from 14-3-3 and interact with Bcl-x and other Bcl2 family proteins located in the mitochondrial membrane. Interaction of Bcl-x with BAD weakens its normal anti-apoptotic activity rendering the cells predisposed to apoptosis. Various studies have shown low level phosphorylated BAD in cells treated with different misfolded proteins and in the brains of mouse models of several neurodegenerative disorders [62;63].

1.6 PRION DISEASE TREATMENT:

At this time there is no effective treatment or cure for TSE [64;65]. The disease is inevitably fatal and affected people usually die within months of the appearance of the first clinical symptoms. Assuming that the hallmark event in the disease is the conversion of PrP^{C} (cellular form of prion protein) into PrP^{Sc}, a reasonable therapeutic target would

be to prevent PrP misfolding and prion replication. This approach has been extensively attempted by many research groups and some compounds have been identified with the capability to decrease prion replication and delay the onset of the clinical disease [5;64]. However, these compounds produce benefit only when they are administered during the pre-symptomatic stage of the disease, long before the appearance of clinical symptoms. It is likely that compounds interfering with prion replication would have little or no benefit to patients with already established clinical disease, since at the time clinical symptoms appear there is substantial brain damage. It seems that a treatment aimed at patients with established symptoms of CJD would need to attack the cellular pathways implicated in brain damage. This is precisely the major goal of my thesis, which originates from my recent studies of the mechanism of neurodegeneration in prion diseases.

1.7 HYPOTHESIS:

Calcineurin plays a pivotal role connecting prion misfolding with synaptic abnormality and neuronal loss, the two major events of prion pathogenesis. My hypothesis is that the sustained increase in cytoplasmic Ca^{2+} , due to chronic ER stress produced by misfolded prion protein, leads to hyper activation of CaN, which finally results in to synaptic dysfunction (in a CREB mediated path way) and neuronal apoptosis (in a BAD mediated pathway). Therefore normalization of CaN activity to the optimum level may be a potential therapeutic strategy against prion disease.

CHAPTER 2

MATERIALS & METHODS [2]

2.1 ETHICS STATEMENT:

All animal experiments were approved by and conducted under strict accordance with guidelines of the Animal Care and Use Committee of the University of Texas Medical Branch in Galveston and the University of Texas Health Science Center in Houston and complied with the recommendations in the Guide for the Care and Use of Laboratory Animals of the National Institutes of Health.

2.2 FK506 PREPARATION:

FK506 was purchased as a powder from LC Laboratories. Purity was >95%. F506 stock solution (0.5 mg/ml) was prepared by dissolving the compound in saline (0.9% NaCl) containing 1.25% PEG40 Castor Oil (Spectrum) and 2% ethanol. FK506 stock solution was stored frozen. Rapamycin (LC Laboratories) was prepared in the same conditions.

[2] A significant amount of this chapter has been previously published in the following article. (Reproduced with permission, see appendix)

Mukherjee,A., Morales-Scheihing, D., Gonzalez-Romero,D., Green,K., Taglialatela,G., and Soto,C. (2010) Inhibition of Calcineurin Activation Increases Survival and Decreases Neurodegeneration at the Clinical Phase of Prion Disease. ***PLoS Pathogens*** 6(10) : e1001138.

2.3 CaN ACTIVITY ASSAY:

The phosphatase activity of CaN was measured using the Calcineurin Cellular Activity Assay kit from Calbiochem as previously described [63]. The brain homogenate were prepared in the assay buffer and the residual phosphate was removed by passing through a desalting column. A final concentration of 1ug/ul of the homogenate was used for the enzyme assay in presence of bovine calmodulin. The reaction mixture was incubated with a final concentration of 150mM RII peptide (substrate) at 37°C for 20 min and reactions were terminated by the addition of 100 µl malachite green reagent. Product formation was measured by recording the absorbance at 635 nm.

2.4 PURIFICATION OF PrP^{C} AND PrP^{Sc}:

As a source of PrP^{C} I used mouse PrP recombinantly expressed in bacteria, purified and folded into the native structure using a previously described protocol[66]. Briefly, the murine *prnp* gene (coding residues 23–230) was PCR-amplified from mouse blood, inserted in a vector and used to transform BL21-Star *E. coli* cells (Invitrogen). For purification, cell pellets were thawed and resuspended, cells were lysed by adding 0.5 mg/mL lysozyme and subsequently sonicated. The released inclusion bodies were pelleted by centrifugation and solubilized in buffer containing 10 mM B-Mercaptoethanol and 6M GdnCl. PrP^{C} was purified by using Ni Sepharose 6 Fast Flow resin (GE Healthcare) in batch-mode. Recombinant PrP^{C} was on-column refolded for 6 h and eluted with 500 mM Imidazole. The main peak was collected and quickly filtered to remove aggregates. The protein was confirmed to be monomeric and folded by size exclusion chromatography, Western blotting and Circular Dichroism.

PrP^{Sc} was purified from the brain of RML scrapie sick mice, following a previously described protocol [67]. Briefly, brains were homogenized in PBS and after a low speed centrifugation, samples were mixed with 1 volume of 20% sarkosyl. Samples were centrifuged at 100,000×g for 3 hr at 4°C. Supernatant was discarded; pellets were resuspended, layered over a 20% sucrose cushion and centrifuged for 3h at 4°C. The supernatant was discarded and the pellet resuspended, sonicated and incubated with PK (100 µg/ml) for 2 h at 37°C and shaking. The digested sample was layered over PBS containing 20% Sarkosyl, 0.1% SB 3–14 and 10% NaCl and centrifuged for 1h 30 min at 100.000×g. The final pellet was resuspended in 100 µl of PBS and sonicated. The sample was stored at −80°C. Purity was >90% as analyzed by silver staining and amino acid composition analysis.

2.5 CELL TOXICITY STUDIES (MTT & LDH ASSAY):

N2A cells were cultured in DMEM supplemented with 10% fetal calf serum and antibiotics (10'000U/ml Penicillin, 10µg/ml streptomycin), at 37°C and 5% CO2. For cell viability analysis, cells were grown in collagen IV coated 96-well plates for 24h in cell culture medium containing 1% serum before addition of the agonist. Cell viability was quantified using 3-(4,5-dimethylthazol-2-yl)-5-3-carboxym ethoxy-phenyl)-2-(4-sulfophenyl)-2H-tetrazolium(MTS) and phenazine methosulfate (PMS) according to the recommendations of the supplier (Promega). Cell death was determined measuring the amount of LDH released to the culture media using the Cytotox 96 LDH kit, following the manufacturer specifications (Promega).

2.6 DETERMINATION OF CYTOPLASMIC CALCIUM:

The changes in intracellular calcium levels were measured 20 minutes after adding the reagents using the Fluo-4 Direct Calcium Assay kit (Invitrogen) in 96 well plate according to manufacturer's protocol.

2.7 ANIMAL MODEL OF PRION DISEASE:

The infectious model of prion disease in mice is a very good model for TSEs, since it reproduces many of the clinical, neuropathological and biochemical aspects of the disease in humans and other mammals [68]. Wild type C57Bl6 mice were injected intraperitoneally (i.p.) with 100µl of brain homogenate containing infectious prions (RML strain). Approximately 210 days after inoculation, animals begin to show signs of scrapie. The disease onset was monitored weekly by visual inspection, using the following scale [69]: 1, normal animal; 2, roughcoat on limbs; 3, extensive roughcoat, hunckback, and visible motor abnormalities; 4, urogenital lesions; and 5, terminal stage of the disease in which the animal presented with cachexia and lies in the cage with little movement. Usually animals die few days after reaching stage 5. The period between the appearance of the first disease symptoms and death ranges between 20–40 days without treatment. Some of the animals were left to die to determine survival time and others were sacrificed at the indicated time by exposure to CO_2 inhalation to assess brain alterations. After animal sacrifice half of the brain was fixed for histological analysis and the other half was kept frozen for biochemical assays.

2.8 ANIMAL TREATMENT:

Treatment with FK506, rapamycin or vehicle was started when animals exhibit the first signs of prion disease (stage 1 in our scale). Animals were injected intra-peritoneally with 0.12 mg of the drug (5 mg/Kg) dissolved in 100 µl of the vehicle solution mentioned above. Administration was done daily until animals die or were sacrificed for experiments.

2.9 ANIMAL BEHAVIORAL TESTS:

To evaluate if treatment with FK506 alters clinical signs we performed open field and rotarod tests. The Open field test monitors exploratory behavior and locomotor activity. Animals were placed in a corner of the field box and all activity during various 20s intervals was recorded by a video camera mounted above the open field and scored in real-time. We measured and analyzed total distance, average speed, time spent in various parts of the field, rearing activity and inactive time. Testing was carried out in a temperature, noise and light controlled room. Rota-rod test is used to measure the motor activity and coordination. Animals were placed on the rotating rod with an accelerated speed (initial velocity 5 RPM; acceleration of 3) and the total time spent on the rod was measured. The animal falls from a high of about 6 inches into a plastic platform that automatically counts the time spent in the rod.

2.10 PrP^{Sc} DETECTION ASSAY:

The presence and quantity of PrP^{Sc} in brain homogenates of sick animals was measured by a standard assay consisting of the ability of the misfolded protein to resist

proteolytic degradation. Samples were incubated in the presence of proteinase K (50 µg/ml) during 60 min with shaking at 37°C. The digestion was stopped by adding electrophoresis sample buffer and protease-resistant PrP was detected by western blotting, as previously described [70]. Briefly, proteins were fractionated by sodium dodecyl sulphate-polyacrylamide gel electrophoresis (SDS-PAGE), electroblotted onto nitrocellulose membrane and probed with 6D11 antibody at a 1:5,000 dilution. The immunoreactive bands were visualized by enhanced chemoluminesence assay (Amersham) and densitometric analysis done by using a UVP image analysis system.

2.11 DETECTION OF pCREB & pBAD:

Frozen brain samples were homogenized in RIPA buffer containing a cocktail of protease inhibitors and were sonicated for 15 s, and then centrifuged at 20,000 g for 5 min. The supernatants were collected and protein concentration measured using BCA assay (Pierce). 50µg of protein extracts were subjected to SDS-PAGE, and western blotting. The membrane was immunoblotted with pBAD, pCREB (Cell signaling; 1:1000) antibodies and the target proteins were subsequently detected using horseradish-peroxidase conjugated anti-IgG secondary antibodies (Amersham Biosciences; 1:2000). Then the membrane was stripped and reblotted with BAD, CREB (cell signaling; 1:1000) to determine the total protein level. In all cases the membrane was reprobed with β-actin (Cell signaling;1:5000) to ensure equal protein loading. As before gels were densitometrically analyzed by the UVP image analysis system.

2.12 POSTMORTEM NEUROPATHOLOGICAL ANALYSIS:

Histological studies were done to assess the effect of the treatment on brain damage. For this purpose half of the brain was fixed in 10% formaldehyde solution, embedded in paraffin and cut in sections using a microtome. Serial sections (8 μm thick) from each block were stained to assess PrP deposition, spongiform degeneration, brain inflammation, neuronal degeneration and neuronal loss. The following studies were done: a) Brain Vacuolation. One of the neuropathological hallmarks of prion diseases is the presence of spongiform degeneration in the brain. Vacuolation was assayed by staining of the tissue with Hematoxilin and eosilin. Then, the number of vacuoles was counted in cerebellum, hippocampus, inferior culliculum, occipital cortex, frontal cortex and thalamus of each animal, as described [69]. b) Brain inflammation. Astrocytosis was assayed by immunohistochemistry utilizing antibodies against Glial Fibrillary Acidic Protein (GFAP) expressed in abundance in activated astrocytes, following a previously described protocol. Staining for activated microglia was done with the AIF-1 antibody. AIF-1 is a 17 kDa interferon-gamma inducible calcium binding protein, associated with chronic inflammatory processes, which has been previously used to assess microglial activation in CJD patients [71]. Digital images were collected on a Leica Microscope fitted with an apotome for optimal sectioning. To calculate the extent of astrocytosis and microglial activation, six 20× sections of Cortex, Thalamus, Hippocampus and Cerebellum were collected per animal and the stained area compared to the total tissue area was determined using the image analysis program Image J from NIH. c) *Neurodegeneration*. To evaluate neuronal degeneration and death I used Fluoro-JadeB

staining to detect degenerative cells and NeuN, a specific marker for neurons. The Fluoro-Jade B staining was done following the protocol described previously[72]. Briefly, 8 µm sections were cut from paraffin embedded brains and spread on microscope slides and allowed to air dry followed by mounting on microscope slides and placed in 70% ethanol. The sections were washed and oxidized by soaking in a solution of 0.06% KMnO4 for 15min. After washing, they were stained with 0.001% Fluoro-JadeB (MiliPore) in 0.1%acetic acid for 20min. Slides were washed again and dried overnight at room temperature. Digital images were collected on a Leica Microscope fitted with an apotome for optimal sectioning. Six 20× sections of Cortex, Thalamus, Hipocampus and Cerebellum were collected per animal. Fluoro-Jade B positive cells were counted from each field. The number of total neurons was counted after staining with the monoclonal anti-NeuN antibody (Chemicon) at 1/1000 dilution. NeuN is a specific neuronal marker for a DNA-binding protein present in the nucleus of postmitotic neurons [73]. Brain sections were mounted onto gelatin-coated coverslips and allowed to air dry. Air dried sections were blocked and permeabilized in 0.1MPB with 0.3% TX-100 (Sigma) and 10% goat serum (PBTGS) for 1 h. Following permeabilization, the mouse monoclonal anti-NeuN antibody (Chemicon International) was applied at a 1:200 dilution and incubated overnight at room temperature. After washing, the secondary antibody and Hoechst (Molecular Probes) were applied for 1 h at room temperature followed by 3 consecutive washes. Slides were visualized under the microscope by two different researchers blinded to the treatment who counted the number of neurons in different brain areas.

2.13 ENZYME ASSAY:

Enzyme master mix was prepared in 2X assay buffer containing 100mM HEPES (Sigma) 1mM DTT (Thermo ; Cat#20291); 1mM CaCl2 (Sigma) 2mM MnCl2 (Sigma; cat # M1787). Calcineurin (EMD cat # 539568) and calmodulin (EMD;Cat # 208964) were incubate in equimolecular ratio (if not otherwise mentioned) for 30 minutes at room temperature. Substrate RIIP (American Peptide; cat # 310258) is dissolved in MilliQ water at 500uM contrition for most of the studies. For Km determination study different concentration of RIIP was prepared by serial dilution of 4mM stock in Mili Q water. Equal volume master mix and substrate was mixed together to initiate the reaction. Reaction was stopped by adding malachite green reagent (Bio Assay System; cat # POMG 25H). Reaction time was determined depending on the assay type. The entire enzyme progress curve was obtained using 0-2hr time scale. Rest of the experiment was performed for 30 minutes. Absorbance of the end product was measured at 620nm using Geminai Spectromax spectrophotometer. For all the enzyme characterization purpose reaction volume was 50ul and malachite green volume was 40ul and for the HTS assay reaction volume was 5ul and malachite green was 2.5ul if not otherwise mentioned. The equations used to fit Km determination curve and CaM titration curve are following.

$$v = \frac{V_{max}[S]}{(Km+[S](1+[S]/Ki))}$$

Where: v= initial velocity, V_{max}= maximum velocity, [S]=substrate concentration, Ki= substrate inhibition constant.

$$Y = \frac{B_{max}[CaM]}{(IC_{50} + [CaM])}$$

Where: B_{max}=maximum CaN activity, [CaM] = calmodulin concentration.

2.14 ENZYME INHIBITION ASSAY:

For the inhibition assay endothall (EMD; cat # 324760) 1.86 mg of the compound was dissolved in 1 ml MilliQ water to prepare a 10 mM stock. Next the stock is serially diluted to 9.5 uM in MilliQ water. 1 ul from each stock was incubated with the master mix for 30 minutes followed by the enzyme reaction imitated by substrate addition. Rest of the reaction condition was kept the same. When the assay was repeated using white plate fluorescent quenching technique the original stock of 10mM was diluted 50 times before starting assay. Percentage inhibition was calculated using formula as follows.

$$\%\,\text{Inhibition} = 100 - \frac{100\,(\text{test well} - \text{average blank control})}{(\text{average DMSO control} - \text{average blank control})}$$

For the reaction was no DMSO is used the denominator is replaced by average positive control.

2.15 MINIATURIZATION OF THE ENZYME ASSAY:

We have first tested the different excitation wavelengths keeping the emission wave length fixed at 610nm on both perkin elmer white cell culture plate and white proxi plates (cat# 6008280) using Geminai SpectroMax EM. Finally we choose excitation at 573nm since it produced maximum emission at 610nm. We also observed that maximum emission changes depending on the plate types. In presence of difference assay solution

the plate was excited at 573nm and fluorescence was measured 610nm. Samples were quenching intrinsic fluorescence of the plate in a concentration dependent manner so that the positive controls produce maximum quenching and the negative controls/blank produce the least. The output from quenching assay was converted in to OD using the following formula.

$$OD = -\,LOG\left[\frac{\text{Signal from test well}}{\text{Average signal from blank}}\right]$$

2.16 STATISTICAL ANALYSIS:

For the *in vitro* studies of the effect of PrP^{Sc} on calcium, CaN activity and cell death, the data was analyzed by one-way ANOVA, followed by the Tukey's Multiple Comparison post-test to estimate the significance of the differences. The *in vivo* survival study was assessed by the Log-rank (Mantel-cox) test. The effect of treatment on the rotarod performance was evaluated by two-ways ANOVA using time and treatment as the variables. The behavioral study by open field test and the differences on CaN activity in animals at different times post-inoculation were evaluated by unpaired t-test (two-tailed). Finally, the effect of treatment on the CaN activity, CREB phosphorylation, BAD phosphorylation, astroglyosis, microglial activation, number of neurons and degenerating cells was analyzed by one-way ANOVA, followed by the Tukey's Multiple Comparison post-test to estimate the significance of the differences. All statistical analysis were done with the GraphPad Prism, version 5.0 software. In the figures the “P-value” is designated in the following way * $P<0.05$; ** $P<0.01$; *** $P<0.001$.

CHAPTER 3

PrP^{Sc}-INDUCED TOXICITY IS MEDIATED BY CaN ACTIVATION [3]

Our previous results showed that PrP^{Sc} accumulation induced ER stress [67]. One of the alterations produced by ER stress is the change of calcium homeostasis. Indeed, exposure of N2A mouse neuroblastoma cells to brain-isolated PrP^{Sc} results in the increase of cytoplasmatic calcium (Fig. 3.1A), which as shown before is coming from the ER[34]. It is well-established that CaN activity is modulated by cytoplasmic calcium concentration. To assess whether neuroblastoma cells exposed to PrP^{Sc} indeed have a higher level of CaN activity, we measured the phosphatase activity in N2A cells treated with 200 nM of PrP^{Sc}. The results show that CaN activity is significantly elevated in cells exposed to PrP^{Sc}, but not to the same concentration of the natively folded recombinant prion protein (PrP^{C}) (Fig. 3.1B). As positive control we used Thapsigargin, an inhibitor of the sarco/endoplasmic reticulum Ca^{2+} ATPase that increases cytoplasmatic calcium concentration [74]. FK506 (also known as Tacrolimus and Prograf) is an FDA approved drug able to inhibit CaN activity [39]. The PrP^{Sc}-induced elevation of CaN activity was efficiently blocked by concomitant addition of FK506 (Fig. 3.1B). To assess the effect of

[3] A significant portion of this chapter has been previously published in the following article. (Reproduced with permission, see appendix)

Mukherjee,A., Morales-Scheihing, D., Gonzalez-Romero,D., Green,K., Taglialatela,G., and Soto,C. (2010) Inhibition of Calcineurin Activation Increases Survival and Decreases Neurodegeneration at the Clinical Phase of Prion Disease. ***PLoS Pathogens*** 6(10) : e1001138.

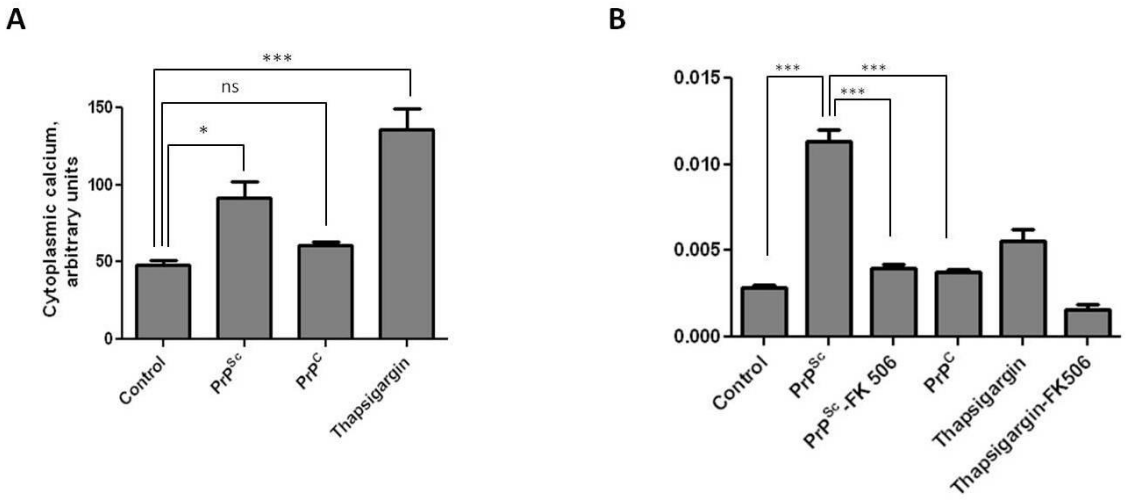

Figure 3.1: PrP^{Sc} induces CaN activation. Panels A, B show the results of in vitro experiments in which 200 nM of purified PrPSc was added to the medium of 1×105 N2A neuroblastoma cells. A, Calcium concentration in cytoplasm was measured after 20 minutes of exposure to PrP^{Sc} using the Fluo-4 Direct Calcium Assay kit in 96 well plate according to manufacturer's protocol. B, Cells were treated for 36 h with 200nM PrP^{Sc} in the presence or the absence of 10µM FK506. As controls, cells were treated with 200 nM of purified recombinant PrP^{C} or with 20µM Thapsigargin (with or without 10 µM FK506). CaN activity was measured using the Calcineurin Cellular Activity Assay kit from Calbiochem according to manufacturer's protocol.

PrP^{Sc} and subsequent CaN activation in cell damage, we measured cell death by release of lactate dehydrogenase (LDH) and cell viability by the MTT (3-(4,5-Dimethylthiazol-2-yl)-2,5-diphenyltetrazoliumbromide) assay in N2A cells exposed to 200 nM of PrP^{Sc} in the presence or absence of FK506 (Fig. 3.2A). Cell death produced by treatment with PrP^{Sc} or thapsigargin was significantly decreased by addition of the CaN inhibitor FK506 (Fig 3.2A). Indeed, the rate of neuroblastoma cell death after treatment with PrP^{Sc} and FK506 was not significantly different from the control untreated cells, indicating that FK506 completely protected cells from PrP^{Sc} toxic activity. A similar protective effect of FK506 against PrP^{Sc} neurotoxicity was found when cell viability was measured by MTT reduction (Fig. 3.2B). To study whether the increase in CaN activity observed *in vitro* as a consequence of PrP^{Sc} formation also occurs under *in vivo* conditions, we measured CaN activity in brain of animals infected with prions. Groups of mice intra-peritoneally infected with the RML prion strain was sacrificed at various time points until the onset of the clinical signs, which under these conditions occurred between 210 and 230 days post-inoculation. A basal CaN activity in brain was detected at all time points during the pre-symptomatic phase, which was not different from the activity found in non-inoculated animals (Fig.3). However, at the beginning of the clinical phase of the disease, a ~3-fold higher CaN activity was found in brain, indicating that the activity of this phosphatase is significantly elevated at the time brain damage and clinical disease occur.

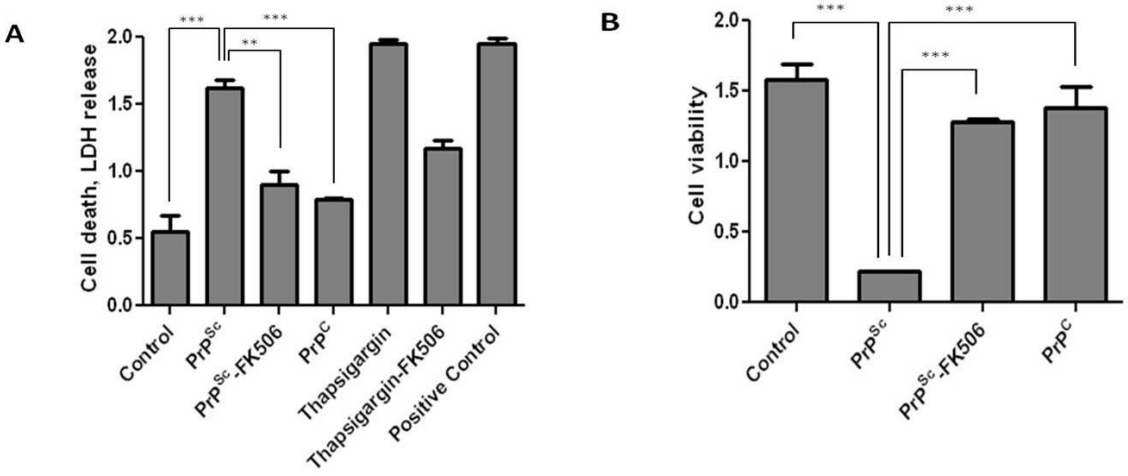

Figure 3.2: PrP^{Sc} induced cell death is rescued by CaN inhibition. Panels A, B show the results of *in vitro* experiments in which 200 nM of purified PrP^{Sc} was added to the medium of 1×10^5 N2A neuroblastoma cells. A,The effect of PrP^{Sc} on cell death or cell viability (B) was measured after 48 hours of incubation (except for the experiment with Thapsigargin that was measured 24 hours after addition of the chemicals). The LDH and MTT assay were performed using the LDH assay kit (Promega) and Cell proliferation assay kit (Roche), respectively, according to the manufacturers' protocol. In case of the cell death assay the positive control, which represents the maximum amount of LDH release, was done by addition of a final concentration of 2% tween20 to the culture medium. All were done in triplicate and the values correspond to the average ± standard error. In these experiments the data was analyzed by one-way ANOVA, followed by the Tukey's Multiple Comparison post-test to estimate the significance of the differences.

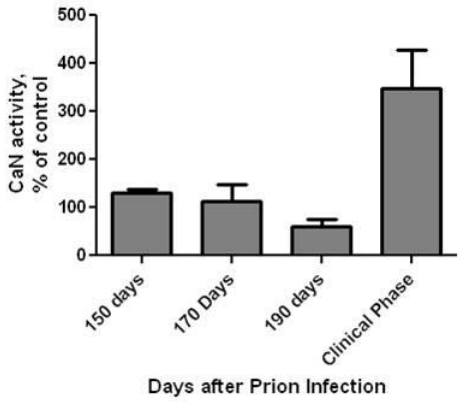

Figure 3.3 Over-activation of CaN at the clinical phase of prion disease mouse model. To study the potential role of CaN in prion diseases I measured the level of CaN activity in animals at different stages of prion disease. For this purpose, groups of 3 mice were sacrificed at different times after i.p. inoculation with RML prions. The brain was collected, homogenized and the CaN activity measured as described in methods. CaN activity is expressed as a percentage of the value obtained in non-infected wild type mice. There were no differences in CaN activity in the brain of control (non-infected) animals during the age range studied (150–250 days). The values used for normalization corresponded to an average of all the animals tested. The differences were analyzed by unpaired student t-test. * $P<0.05$; ** $P<0.01$; *** $P<0.001$.

CHAPTER 4

OPTIMIZATION OF CaN ACTIVTY INHIBITS PRION DISEASE PROGRESSION IN MOUSE MODEL [4]

To study the potential role of CaN in prion-induced neurodegeneration and to assess the possibility of inhibiting this phosphatase as a putative target for therapeutic intervention, I treated prion infected animals with the FDA-approved CaN inhibitor FK506. FK506 (also known as Tacrolimus and Prograf) is a natural product produced by the fungus Streptomyces tsukubaensis, marketed to prevent transplant rejection [75]. By inhibiting CaN, the drug suppresses both humoral and cellular immune responses [39]. Our results show that mice receiving FK506 after the onset of the clinical phase of prion disease exhibited improved motor activity and coordination, lived longer and had a decreased level of brain degeneration when compared to untreated prion infected animals. These findings suggest that inhibition of CaN activity in the brain may be a promising new approach for the treatment of prion diseases.

[4]A significant portion of this chapter has been previously published in the following article. (Reproduced with permission, see appendix)

Mukherjee,A., Morales-Scheihing, D., Gonzalez-Romero,D., Green,K., Taglialatela,G., and Soto,C. (2010) Inhibition of Calcineurin Activation Increases Survival and Decreases Neurodegeneration at the Clinical Phase of Prion Disease. ***PLoS Pathogens*** 6(10) : e1001138.

4.1 INHIBITION OF CaN ACTIVITY DECREASES DISEASE SEVERITY AND INCREASES ANIMAL SURVIVAL:

To study whether CaN activity is implicated in the progression of prion disease and whether the inhibition of this phosphatase could be a good target for therapy, groups of mice were treated with FK506 during the clinical phase of the disease. Clinical onset of the disease was carefully measured every other week by two different researchers monitoring the appearance of hunch and trail rigidity, which is the first alteration clearly associated to the disease. When the clinical symptoms were unambiguously observed during 3 consecutive days, infected mice were injected i.p. daily with 5 mg/kg of FK506 (dissolved in saline, containing 1.25% PEG40 Castor oil and 2% ethanol) (n = 14) or with vehicle (n = 14). This dose was chosen based on a toxicology study showing that administration of FK506 at concentrations higher than 10 mg/Kg produced side-effects detectable by behavioral tests. As a control I used another immunosuppressant drug, Rapamycin (n = 8), which does not interfere with CaN activity. Treatments lasted until animals died or were sacrificed for analysis. Progressive decline in motor coordination and activity is a well documented clinical feature of prion disease, which likely is the result of loss of synaptic integrity. Therefore motor alterations during the clinical phase

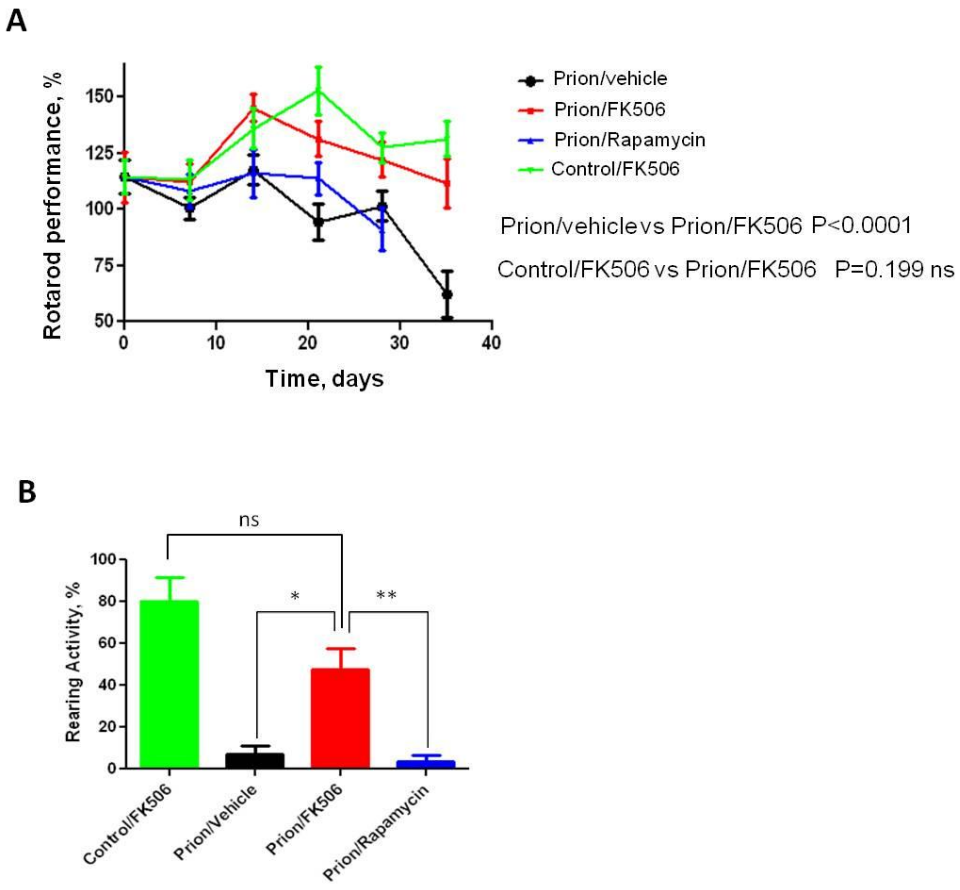

Figure 4.1: Inhibition of CaN reduces disease progression. Animals were treated daily with 5 mg/Kg of FK506, rapamycin or vehicle (the buffer used to dissolve FK506) starting at the time they exhibited the first signs of prion disease. Behavioral and motor alterations were measured over time by Rota-rod (**A**) or open field (**B**) tests and compared with age matched wild type animals treated with FK506. Activity was assessed once a week and the initial performance (t = 0) was normalized with respect to the age matched wild type non-infected animals. The locomotor activity in the rota-rod test was measured by placing mice on the rotating rod with an accelerated speed and the total time spent without falling was recorded. The rearing activity in the open field box was measured as the number of times the animal spent in vertical activity during 20s intervals. The graph in panel B shows the results obtained at 21 days after beginning of the treatment. Each value corresponds to the average and standard error (n = 4 for rapamycin and n = 10 for other groups).

of the disease in animals treated with FK506, rapamycin or vehicle were assessed by using rota-rod (Fig. 4.1A) and open field tests (Fig. 4.1B). The motor coordination in the rota-rod test was measured once a week in a 3 min. time interval and was expressed as a percentage of the activity at day 0 (day in which treatment was started). The results showed that prion infected animals treated with vehicle or rapamycin experienced a progressive and significant decline on motor coordination, whereas animals treated with FK506 showed no significant decrease on performance over the 5 weeks period (Fig. 4.1A). Indeed, the rota-rod performance of the FK506 treatment group was similar to that of non-infected animals (either treated or untreated with FK506), used as control. The slight increase on performance over the time period in control animals probably reflects that animals become more familiarized with the test. The locomotor ability in open field test was measured at day 21 after starting the treatment, by the rearing activity during 20s and corresponds to the time animals spent only on the hind limb. As shown in Fig.4.1B, the rearing activity in prion infected animals was dramatically reduced compared to control non-inoculated animals. Treatment with FK506, but not rapamycin, prevented significantly the locomotor deficiencies. Next I investigated the survival time of the animals under treatment. Infected mice were left to die naturally and time of death was recorded. Fig.4.2 shows the survival curve of the group treated with FK506 (n = 10, red line), treated with rapamycin (n = 4, blue line) or the vehicle group (n = 10, black line). The results showed a 35% increase in survival of the group treated with CaN inhibitor compared to the vehicle treated control (P = 0.039, as estimated by the Log-rank Mantel-cox test).

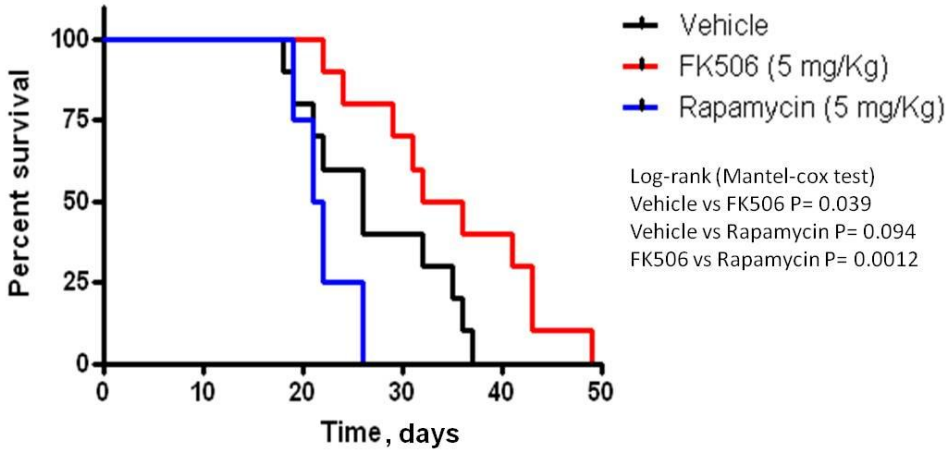

Figure 4.2: Increase in survival of prion infected animals by treatment with CaN inhibitor. Animals were treated daily with 5 mg/Kg of FK506, rapamycin or vehicle (the buffer used to dissolve FK506 and rapamycin) starting at the time they exhibited the first signs of prion disease. Groups of animals were left to die to determine survival time in each condition. FK506 treated mice (n = 10, red line; average symptomatic phase: 35±2.8 days), treated with rapamycin (n = 4, blue line; average symptomatic phase: 20.9±0.9 days), vehicle group (n = 10, black line; average symptomatic phase: 26.2±2.2 days). Differences were analyzed by the Log-rank (Matel-cox) test.

4.2 FK506 TREATMENT DOES NOT ALTER PrP^{Sc} ACCUMULATION BUT INCREASE pCREB AND pBAD:

To study the effect of FK506 treatment on neurodegeneration, 4 random animals from each treatment group were sacrificed at the time in which the first mice injected with vehicle reached the stage 5 of the clinical disease (around 20 days after the beginning of the treatment), their brains were collected and one hemisphere was kept frozen and the other fixed for histological analysis (see below). Frozen brains were homogenized in TBS with protease inhibitors. The level of CaN activity in total brain

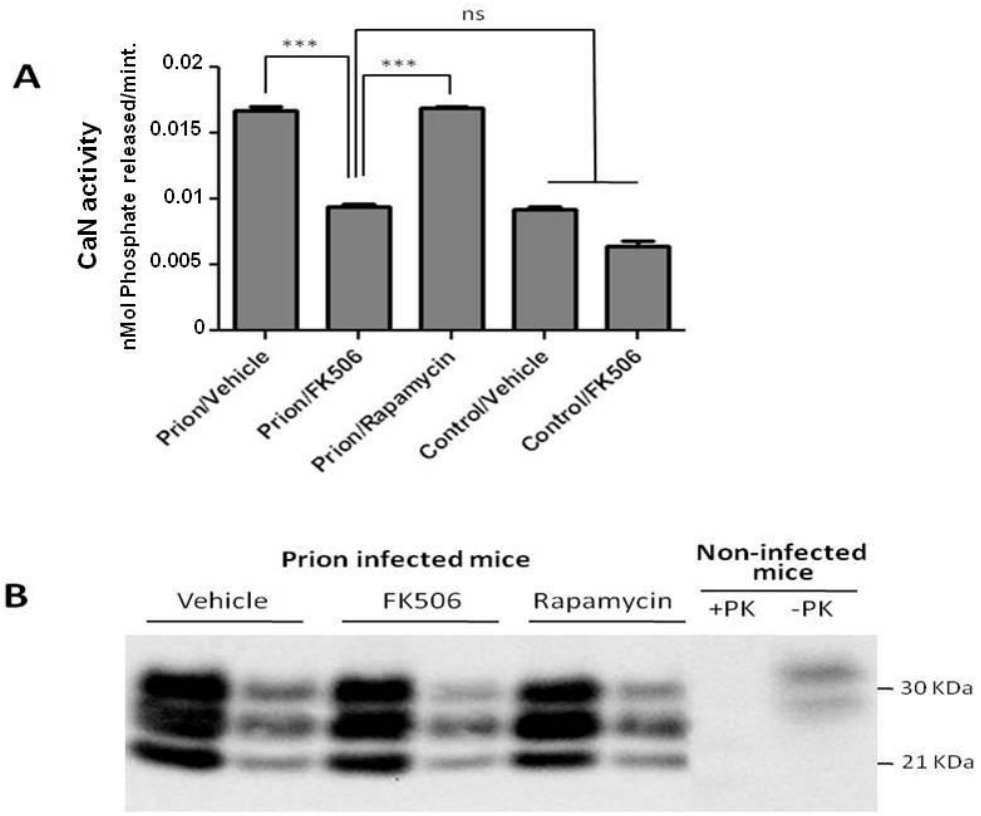

Figure 4.3: Effect of FK506 treatment on PrP^{Sc} formation and CaN activity.

To study the effect of the treatment on neurodegeneration, 4 random animals from each treatment group were sacrificed when mice injected with vehicle reached the stage 5 of the clinical disease. Their brain was collected and one hemisphere was kept frozen for biochemical studies. As controls we used age-matched non-infected animals that received either vehicle or FK506. **A**, levels of CaN activity were measured as described in methods. The values represent the average ± standard error of 3 determinations. **B**, PrP^{Sc} accumulation was determined by western blot after PK digestion as described in methods. For each condition, the western blot of a representative animal is shown in two dilutions (5 and 25 fold dilution of 10% brain homogenate). Normal mouse brain homogenate treated in the same way with or without PK digestion was also loaded.

was measured as described in methods. Prion inoculated mice had substantially higher CaN activity in the brain of inoculated mice (Fig. 4.3A), supporting the result shown in (Fig. 3.3) The levels of CaN activity in prion inoculated mice were normalized upon treatment with FK506, indicating that the drug is acting as expected in the brain and that the dose used was appropriate.

To measure PrP^{Sc} accumulation in the different group of animals, samples were treated with PK (50 µg/ml for 1h at 37°C) and 1/5 and 1/25 dilutions from the 10% brain homogenate were evaluated by western blot. The result shows that FK506 treatment did not alter PrP^{Sc} accumulation (Fig. 4.3B), a result consistent with our hypothesis that CaN activation is a downstream event of prion replication. To study the influence of CaN inhibition in the phosphorylation stage of some of the key substrates of the phosphatase involved in controlling synaptic plasticity and neuronal apoptosis, we measured the brain levels of pCREB, pBAD as well as total CREB and BAD. The western blot in Fig.4.4A shows the result of CREB of two representative animals per group and the graph in the right panel represents the quantification of the ratio pCREB/total CREB. The results indicate that scrapie-affected mice receiving vehicle have a 2-fold reduction of pCREB (normalized to total CREB) compared to non-infected animals. Strikingly, treatment with FK506, but not rapamycin, restored the concentration of this phosphorylated transcription factor to reach levels indistinguishable from healthy controls (Fig. 4.4A). A similar result was observed when the pro-apoptotic BAD protein was analyzed. Indeed, prion affected mice have a 3–4 fold reduction of pBAD/total BAD ratio compared to controls. Again,

the phosphorylation state of this important protein was restored upon treatment with FK506 (Fig. 4.4B).

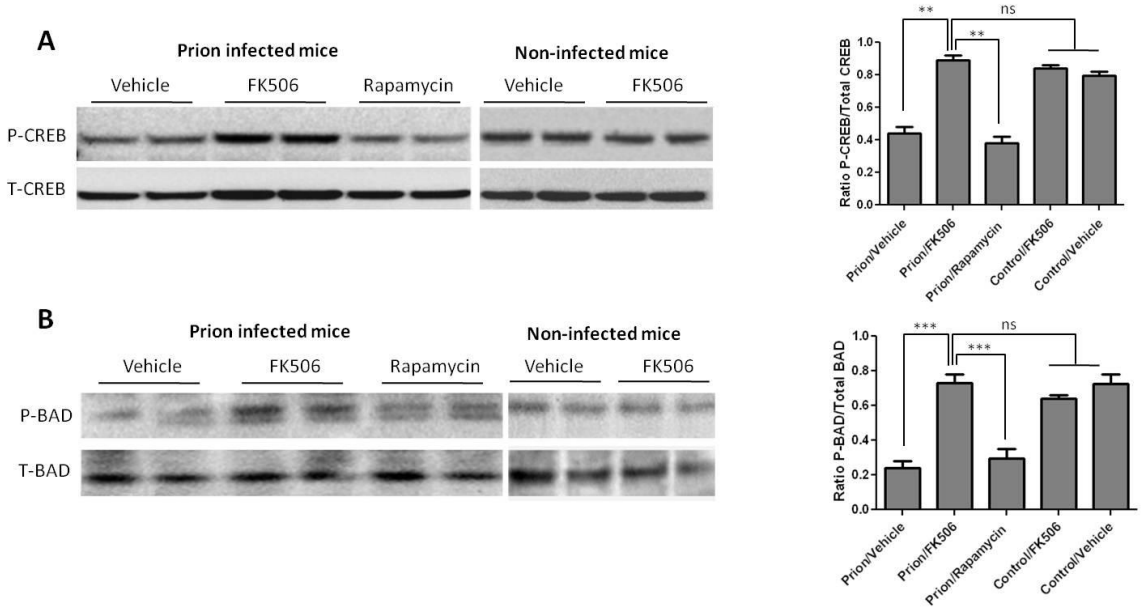

Figure 4.4: Recovery of pCREB and pBAD level by optimization of CaN activity.

A, The brain levels of pCREB and total CREB were determined by western blots in animals infected with prions and treated with vehicle, FK506 or rapamycin, as well as in non-infected age-matched mice treated with vehicle or with FK506. The blot shows the results of 2 different animals per group and the graph in the right side displays the densitometric analysis of the 4 animals studied in each condition. The values correspond to the average ± standard error. B, The levels of pBAD and total BAD were estimated by Western blot and the data densitometrically analyzed. As before, the values in the graph correspond to the average ± standard error of 4 animals per group. For the western blot analysis, the same total protein concentration was loaded in each lane and equal loading was additionally confirmed by developing the membrane with anti-actin antibody. The data was statistically analyzed by One-way ANOVA followed by the Tukey's Multiple comparison post-test. * $P<0.05$; ** $P<0.01$; *** $P<0.001$.

4.3 ASTROGLIOSIS AND MICROGLIOSIS WERE NOT ALTERED BY CaN INHIBITION:

To further assess the effect of FK506 treatment on prion induced neurodegeneration, fixed brains from 4 animals per group were stained and analyzed. The histopathological alterations observed in prion affected animals, include spongiform degeneration, astroglyosis, neuronal death and synaptic dysfunction. Analysis of the extent of vacuolation revealed no significant differences between treated and un-treated animals. Although, spongiosis is the most characteristic brain alterations observed in TSEs, its role in brain dysfunction and clinical disease is mostly unclear [76;77]. Brain inflammatory changes in the form of reactive astrocytes and activated microglia are also a typical alteration associated to prion diseases [78]. Since CaN has been implicated in immunological and inflammatory pathways [79], we wanted to analyze in detail the effect of FK506 treatment on the extent of astrocytosis and microglial alteration. Astrogliosis was studied by staining the tissue with the anti-GFAP (glial fibrillary acidic protein) antibody and reactive microglia with the anti-AIF1 (allograph inflammatory factor 1) antibody (Fig. 4.5A). Quantification of the area of the thalamus containing reactive astrocytes (Fig. 4.5B) and activated microglia (Fig. 4.5C) revealed a pronounced difference between samples coming from non-infected and prion infected animals. However, no statistically significant differences on the extent of brain inflammation were observed among prion infected animals treated or untreated with FK506 or rapamycin.

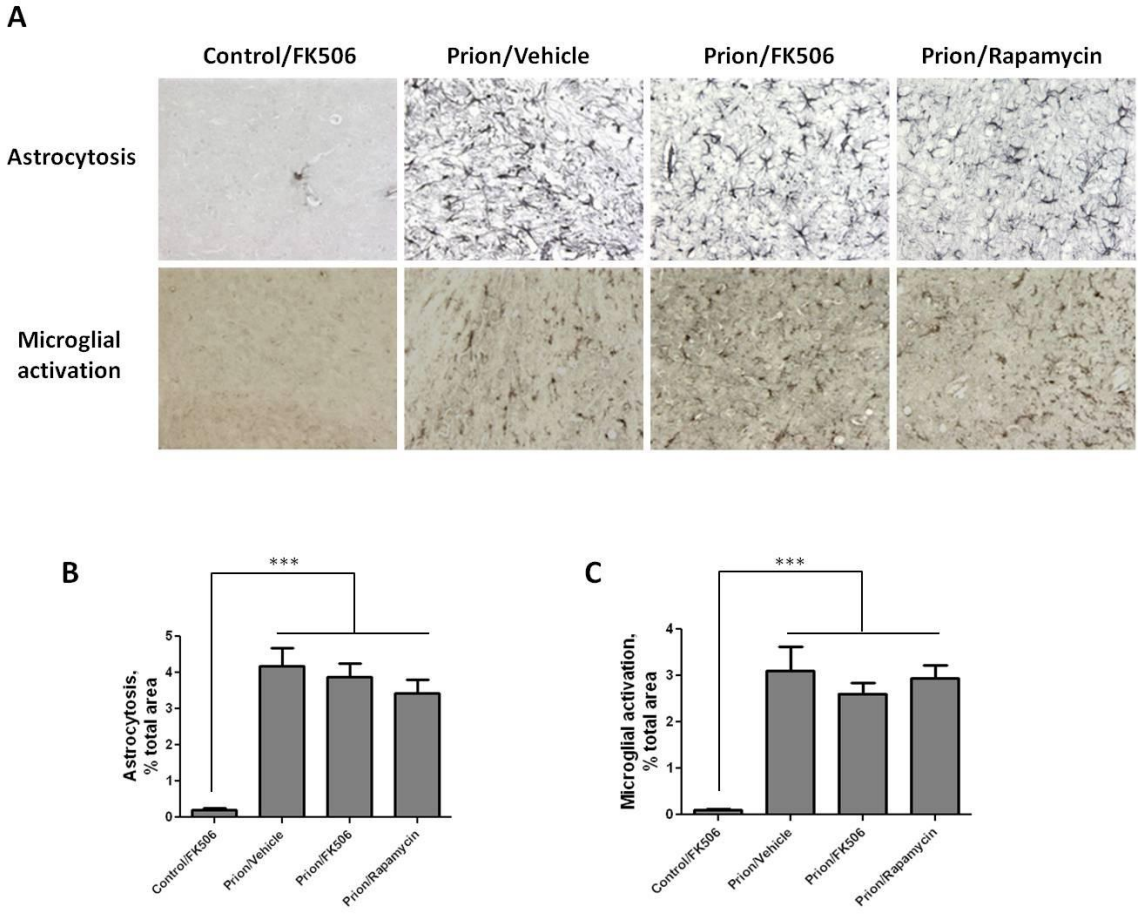

Figure 4.5: Unaltered astrogliosis and microgliosis after FK506 treatment.

The number of neurons in various brain areas of mice infected or non-infected with prions and subjected to diverse treatments was evaluated by histological analysis using the Neu-N antibody, which specifically recognizes neuronal cells. **A**, representative pictures of the thalamus region after staining with Neu-N (brown) and Hoesch (blue) to stain nucleus. We focused on thalamus, because this is one of the brain areas most severely affected in RML-affected animals. **B**, to quantitatively assess the number of neurons in different groups we randomly selected two different regions of thalamus in each animal and two investigators blinded to the treatment counted the number of neurons using the image pro software. In prion infected animals we observed some abnormal immunoreactivity in the form of elongated structures. We believe this staining represents degenerated nerve cells process or cellular debris. We did not consider these immunoreactivities in the neuronal counting. Each value corresponds to the average and standard error (n = 3 for rapamycin group, and n = 4 for all other groups). The data was

statistically analyzed by One-way ANOVA followed by the Tukey's Multiple comparison post-test. * $P<0.05$; ** $P<0.01$; *** $P<0.001$.

These results suggest that the therapeutic effect of FK506 is not mediated by a neuroimmune pathway.

4.4 REDUCTION OF NEURODEGENERATION BY CaN INHIBITION IN PRION AFFECTED MICE:

To study the number of neurons present in the brain, we stained tissue slides with NeuN, a specific and well-established neuronal marker [73]. The data shows a substantially higher quantity of neurons in the thalamus of FK506 treated-mice, compared with prion affected animals treated with vehicle or rapamycin (Fig. 4.6). Indeed, mice treated with the CaN inhibitor have almost twice the number of neurons as their untreated-mates. However, still the treated animals have around 50% less neurons than normal animals not affected by prion diseases (Fig. 4.6), indicating that the treatment only stops in part the neurodegeneration process. In order to further study the influence of the treatment on neuronal damage, we stained the tissue with Fluoro-Jade, a well-established method to detect degenerating neurons[80]. As shown in Fig. 4.7, the brain of mice treated with FK506 has a substantially lower level of Fluoro-Jade stained cells as compared to animals treated with vehicle or rapamycin. Again, the effect of the treatment was not complete, since FK506 treated mice still have significantly more degenerating neurons than the control non-infected animals (Fig. 4.7).

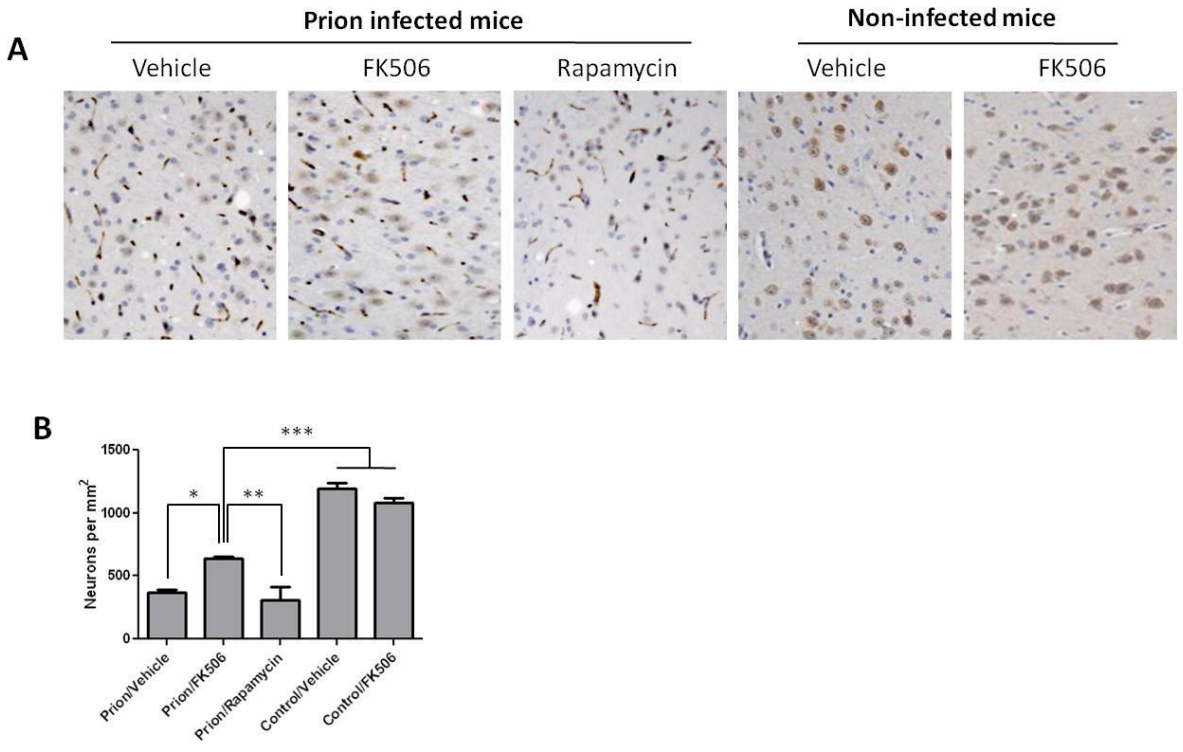

Figure 4.6: Treatment with FK506 decreases prion-induced neuronal loss:

The number of neurons in various brain areas of mice infected or non-infected with prions and subjected to diverse treatments was evaluated by histological analysis using the Neu-N antibody, which specifically recognizes neuronal cells. **A**, representative pictures of the thalamus region after staining with Neu-N (brown) and Hoesch (blue) to stain nucleus. We focused on thalamus, because this is one of the brain areas most severely affected in RML-affected animals. **B**, to quantitatively assess the number of neurons in different groups I randomly selected two different regions of thalamus in each animal and two investigators blinded to the treatment counted the number of neurons using the image pro software. In prion infected animals I observed some abnormal immunoreactivity in the form of elongated structures. I believe this staining represents degenerated nerve cells process or cellular debris. I did not consider these immunoreactivities in the neuronal counting. Each value corresponds to the average and standard error (n = 3 for rapamycin group, and n = 4 for all other groups). The data was statistically analyzed by One-way ANOVA followed by the Tukey's Multiple comparison post-test. * $P<0.05$; ** $P<0.01$; *** $P<0.001$.

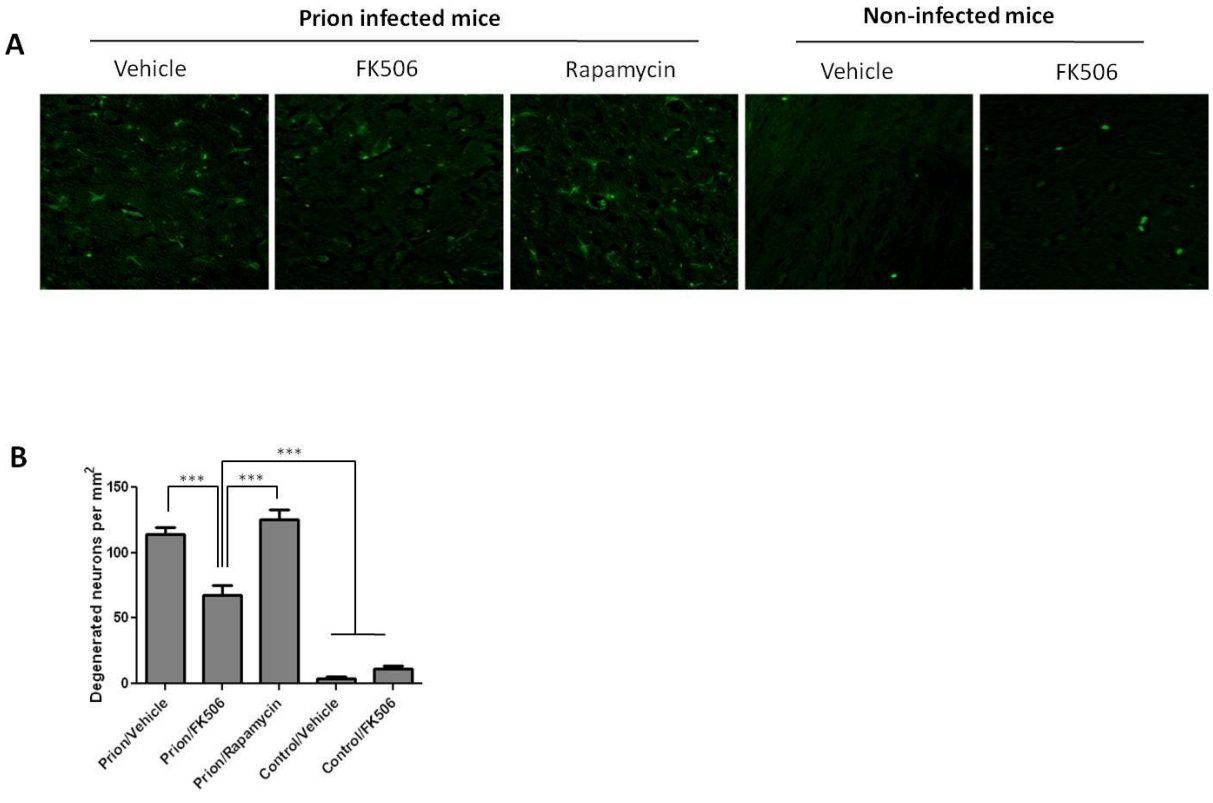

Figure 4.7: CaN inhibitor reduces neurodegeneration in prion infected animals.

Nerve cell degeneration was studied by Fluoro-Jade staining in thalamus sections and visualized by fluorescence microscopy. Panel **A** shows representative pictures from several animals (3 for rapamycin, 4 for the other groups) and panel **B** shows the number of degenerating neurons in each group. The data was statistically analyzed by One-way ANOVA followed by the Tukey's Multiple comparison post-test. *** $P<0.001$.

CHAPTER 5

DEVELOPMENT OF A ROBUST ASSAY TO SCREEN NOVEL INHIBOTORS AGAINST CaN

Perhaps, one of the reasons that contributed towards the partial efficiency of the treatment is the low penetration of FK506 across the blood-brain barrier. In order to observe an effect *in vivo* in the Central Nervous System (CNS) the doses have to be very large, increasing the extent and severity of side effects. Therefore it is necessary to find an inhibitor for CaN with improved pharmacokinetic properties blood brain barrier permeabilty. In order to further develop our therapeutic strategy I have been awarded with NIH/NINDS Cooperative agreement award (U24) to conduct high throughput screening (HTS) of drug-like small molecules against CaN in Harvard Neuro Discovery Center. Here I describe development of a high-throughput compatible assay to screen for small molecule inhibitors of CaN.

5.1 CHARACTERIZATION OF CaN ENZYME ACTIVITY:

To develop a specific and CNS directed CaN inhibitor I decided to target CaN-CaM binding site. This site is unique for CaN compared to other phosphatases and this binding is required for CaN activation as well. The Km_a value of CaN was determined in presence of molar excess CaM, using RIIP as a substrate. The value determined was

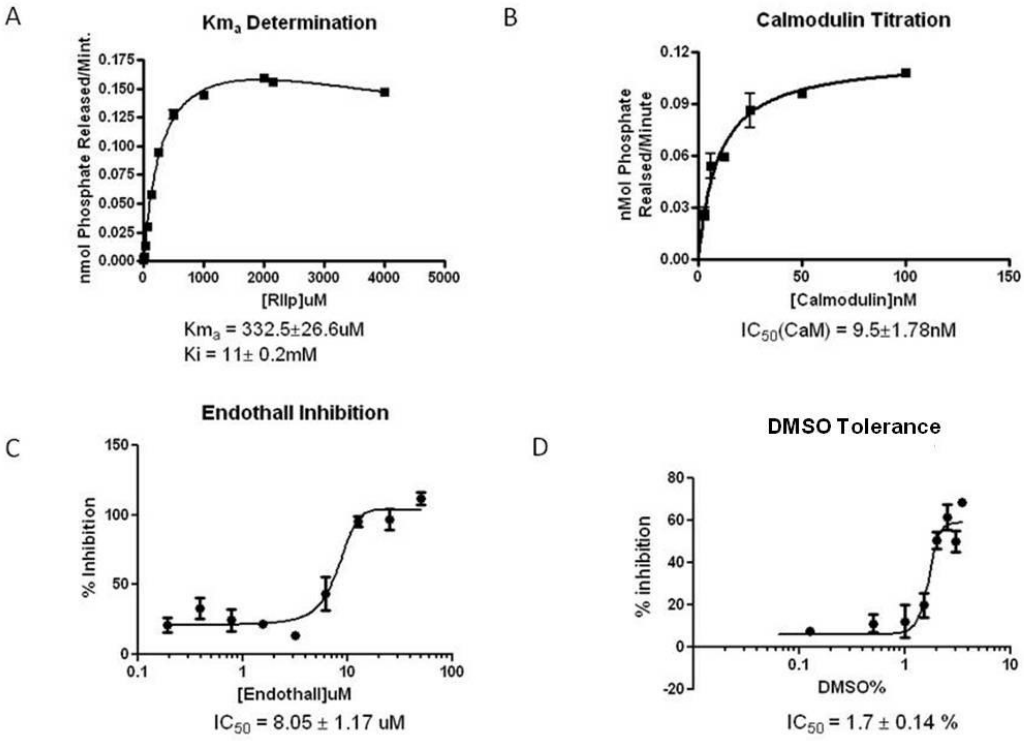

Figure 5.1: Characterization of Enzyme Activity. In all the assays the concentration of CaN and CaM were 10nM. The data points represent average and standard deviation of reaction done in triplicate. The fittings are done using prizm software. Details are mentioned in method section. A, Km_a was determined by plotting initial velocity at different substrate (RIIP) concentration. The calculated Km_a value is 332 ± 26.2 uM. B, The concentration of CaM which produces 50% activation (IC_{50}CaM) of CaN is determined by plotting initial reaction velocities at different CaM concentrations keeping the substrate concentration constant at 300uM. Our data indicates CaM produces half maximum CaN activity at 1:1 molecular ratio. C, Represents the endothall inhibition curve. The calculated IC50 is 8.05 ± 1.17uM. D, Represents DMSO tolerance curve. The data indicate that we can up to 1% DMSO without losing CaN activity.

332uM which is very similar to the one published before [81] (Fig.5.1A). Substrate inhibition was repeatedly observed while determining Km_a which was not previously reported for CaN. CaM titration study, in presence of molar excess of Ca^{2+} , indicated that molar ratio of 1:1 (CaN:CaM) produces 50% activation of CaN (Fig.5.1B). For this reason, the next set of experiments were carried out at 1:1 molar ratio of CaN /CaM aiming to develop a specific inhibitor of CaN which will not interfere with the activity of other phosphatases. Optimum Ca^{2+} was also determined to produce maximum activity with a fixed concentration of CaN/CaM. It has been reported that there is a binuclear metal center in the active site of CaN which binds to negatively charged phosphate ion during the catalysis [81]. Therefore bivalent metal ions like Mg^{2+} and Mn^{2+} were tested. The result indicates that Mn^{2+} at 1mM concentration produces maximum CaN activity, whereas Mg^{2+} does not produce any effect. Proper oxidation state of the divalent cations is also essential for the catalytic activity of CaN rendering the active site prone to oxidative damage. Therefore I used DTT in our assay and found that 500uM of DTT was enough to produce maximum activity. Next pH titration was performed and results indicated that pH 7.0 was optimum for the assay. Once the assay parameters were characterized endothall, a known inhibitor of calcineurin, was tested in my assay system. The published IC 50 value was faithfully replicated (Fig. 5.1C). DMSO tolerance of CaN has also been performed since the entire compound library that had to be tested was in DMSO. The data indicate that the enzyme can withstand up to 1% DMSO in our assay setting (Fig. 5.1D).

5.2 TECHNICAL STANDARDIZATIONS:

Once the assay parameters were established, I proceeded to test technical conditions that are critical for HTS. First the effect of freeze-thaw and the binding property of

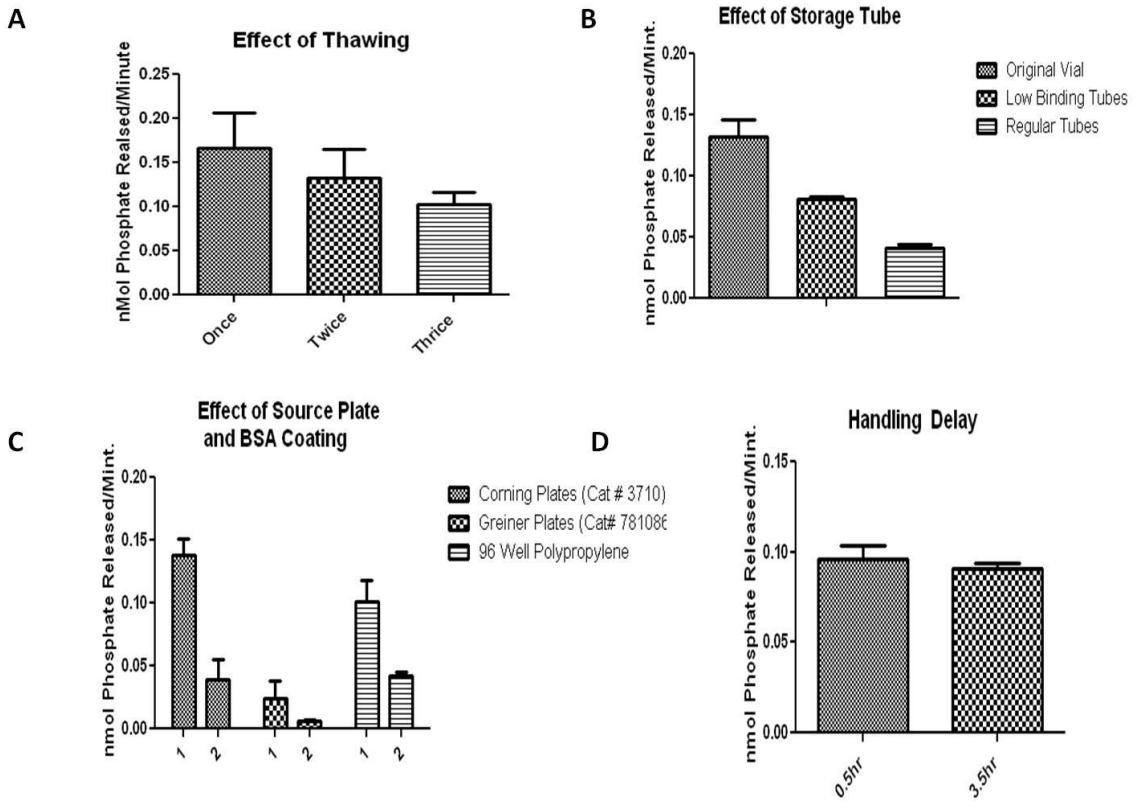

Figure 5.2: Technical standardizations. In all the assays the concentration of CaN and CaM were 10nM and RIIP were 300uM. The data points represent average and standard deviation of reaction done in triplicates. A, Represents the effect of thawing on CaN activity. After receiving the fresh vial from the vendor it was thawed on ice and activity was measured. This is considered "thaw once". Next it was frozen in liquid N_2 and kept in -80C for overnight followed by thawing the vial next day. This is considered "thawed twice" and so on. The data indicate that there is significant effect of thawing on CaN activity. B, Represents the effect of different storage condition on the enzyme. After

receiving the fresh vial from the vendor it was thawed and aliquoted in different tubes including the vial it came: “original vial” followed by fast freezing in liquid. Aliquots were kept in -80C over night and the next day activity was measured. The result suggests it is always better to store the enzyme in the original vial. C, Represent the effect of different source plates on enzyme activity with and without BSA coating. 1: coated with 1mg/ml BSA; 2: uncoated plates. According to result the BSA coating is always beneficial irrespective of the plates. D, Represents the effect of handling delay on the master mix containing CaN. 50ul of the master mix was kept in 96 well polypropylene plate at RT with a lead. Next the enzyme activity was measured at different time points.

the enzyme with common storage device and assay platforms were tested. This is important since losing activity due to freeze-thaw or unspecific binding may greatly influence the result in an HTS assay. The enzyme can withstand 2 consecutive freeze thaw cycle if always kept in the same vial (Fig. 5.2A). However, if it is aliquoted in different tubes, including low binding tubes, CaN significantly loses activity. (Fig. 5.2B). For an HTS enzymatic assay, normally the enzyme mix is kept in a 384 well plate which is used as an enzyme source plate to expedite the liquid handling. Since my data suggests significant unspecific binding of CaN, I tested different plates which may be used as source plates during automated screening. The data indicated that in presence of BSA coating all the plates behaved similarly except greiner plates. However, without coating there is significant lose of CaN activity (Fig. 5.2C). Normally it is advised to set an HTS assay with minimal required components. However, in this case coating of the plate may be essential. Since calcineurin is susceptible to oxidative damage my concern was it may lose activity when kept in the source plate wells for duration of liquid handling. To estimate a safe time window, while the enzyme can be kept without any loss of activity, I have mimicked the condition of original HTS screening. The enzyme master mixture was

kept in the source plate and at different time points aliquots were taken to run the reaction. The result indicates that the enzyme can be kept at least for 3 hours in the source plate without any damage (Fig. 5.2D).

5.3 MINIATURIZATION OF THE ASSAY:

After standardization of all the parameters and conditions the assay was transferred from 96 well format to 384 well format which is suitable for HTS. Although absorbance assays are simple, the reading depends on the path length requiring higher assay volume even in a 384 well format. On the other hand, fluorescent assays are more sensitive with volume <10ul which is ideal for HTS assay. Therefore I decided to convert malachite green based absorbance assay into a fluorescent assay using white plate fluorescent quenching technique [82]. White 384 well perkin elmer cell culture plates were shown to have substantial background fluorescence with broad emission spectra. The background fluorescence emission was utilized to measure intensity of green color (absorb at 610nm) produced by malachite green upon binding to inorganic phosphate. The emission wavelength of the empty wells was selected at 610nm so that the emitted light can be efficiently absorbed by the phosphate malachite green complex and the quenching of the signal can be measured which was proportional to the product formed. Next, the reading was converted in to OD using the formula described in the method [83].

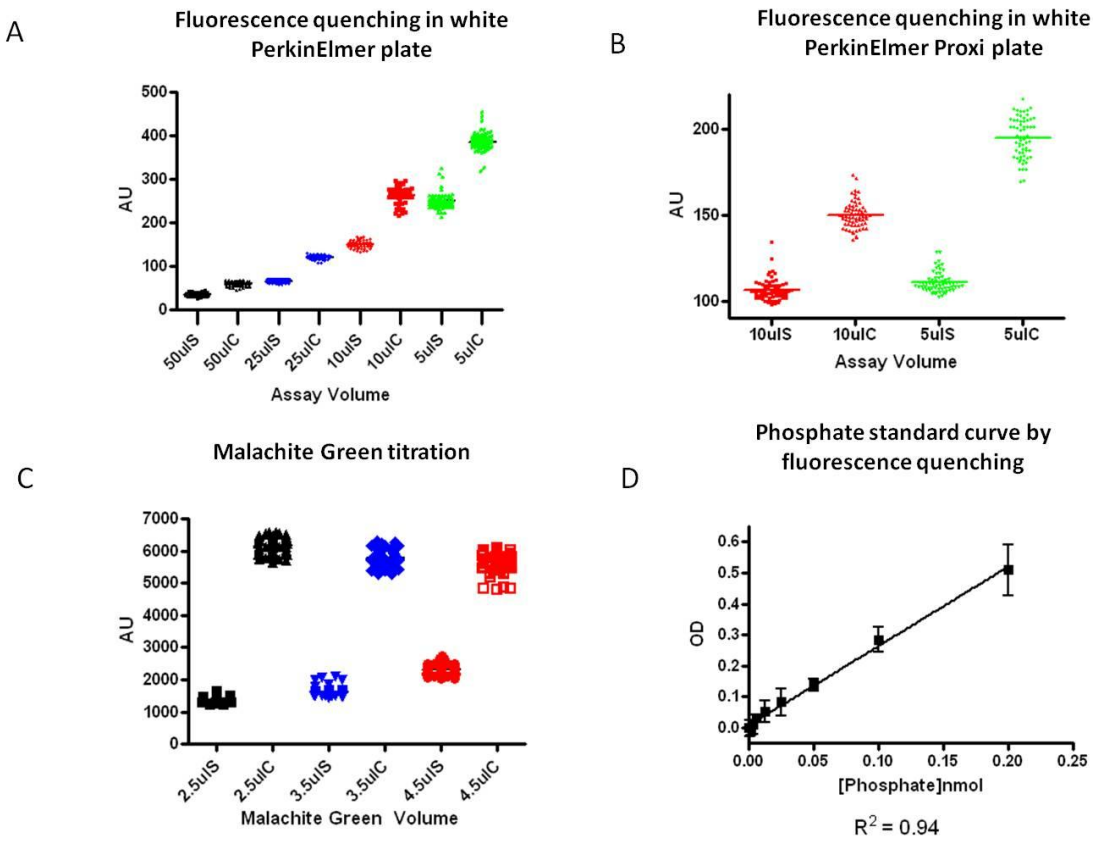

Figure 5.3: Miniaturization of the assay. In this figure the raw data is presented instead of OD unless otherwise indicated. 80 wells were used to generate each data set. A, Different volumes of standard solution contains 0.25nmol phosphate (sample: s) and the corresponding buffer solutions (control: c) were added to 384 perkin elmer white culture plate. The color codes for the volumes are: 50ul : black; 25ul : blue; 10ul : red; and 5ul : green. The malachite green volume was kept at 1.25:1 ratio. B, Represents the same experiment done in low volume white proxi plates using 5 and 10ul of developing reagent. C, malachite green titration keeping the assay volume constant at 5ul. The color codes are 4.5ul : red; 3.5ul : blue and 2.5ul : black. D, represents a phosphate standard curve generated using white plate fluorescence quenching. The result indicates that the 5ul assay volume with 2.5ul developing reagent produces the optimum result using white proxy plates.

Using this technique the reaction volume was titrated keeping the phosphate concentration constant at 0.25 nmol/well in order to determine a volume which produces maximum sensitivity (difference in the average positive and negative control). The result indicated that sensitivity increases with the reduction in volume (Fig. 5.3A), with 5ul assay volume producing the best result. However with lower volume more dispersion of the data was noted. To lower the variability of the data set I decided to use white proxi plates suitable to work with lower volume. With this new plate assay volume up to 5ul was tested and as expected the new plates increased the sensitivity (Fig. 5.3B). I deliberately did not go beyond 5ul assay volume since it will be difficult for the robotic system to handle. Next, the developing reagent was titrated keeping the assay volume constant. The data indicate that 2.5ul malachite green produces maximum sensitivity (Fig. 5.3C). After standardizing the assay and developing reagent volume a phosphate standard curve was prepared using the current settings (Fig. 5.3D). Conversion of the assay from absorbance to a fluorescence based assay produced high sensitivity at low phosphate concentration range which can no way be achieved using regular absorbance assay. Next, linearity of the assay is determined using different enzyme concentrations. The result suggests that 5nM CaN was enough to produce robust signal within the linear range of phosphate standard curve.

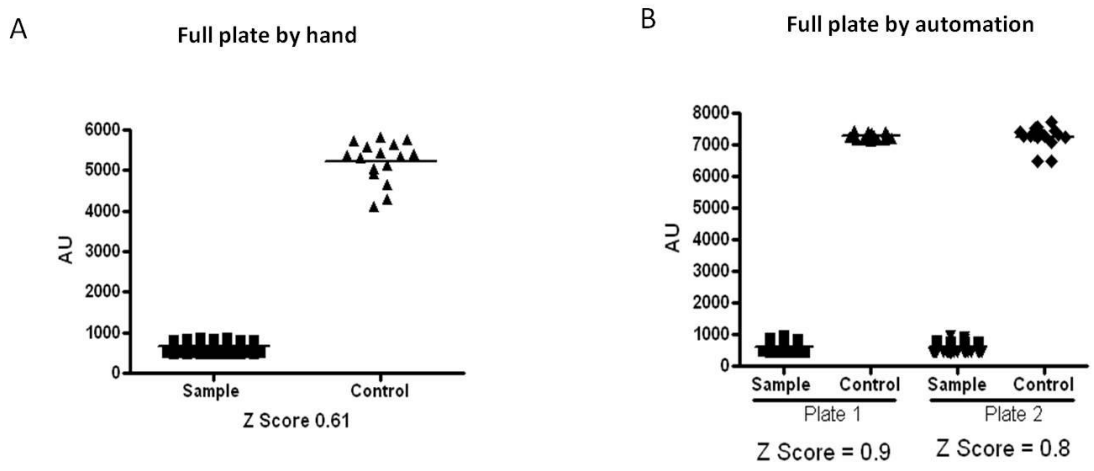

Figure 5.4: Validation of the assay. A, Represents complete assay in a full plate without using automated liquid handling. The term sample represents the reactions where enzyme master mixture was incubated 30 minutes with 300uM RIIP followed by detection with malachite green. Control represents the wells where master mixture was replaced by the corresponding buffers. B, Represents the same experiment as in C, done in 2 different full plates using automated liquid handling system.

5.4 AUTOMATION OF THE ASSAY:

Since the white plate fluorescent quenching technique was faith fully replicating all the results obtained using the absorbance assay I went ahead and studied the Z score and the CV of a full 384 well plate done by hand. The statistical parameter "Z score" represents the range of separation window between the dynamic ranges of positive negative control values. The value ranges form 0-1. Z score over 0.5 is normally considered excellent for an HTS assay. In our manual version of the assay we reached Z score of 0.61 (Fig. 5.4A). CV which reflects the variability between replicates should not exceed 20% for a good HTS assay. I obtained 15% for the positive controls and 10% negative controls. After satisfying all the statistical requirements to generate highly reproducible and robust assay I moved on to automated screening procedure. Using our robotic system I have performed the assay in 2 full plates. The Z score value was ranging within 0.8-0.9 (Fig. 5.4B) implicating that with automated liquid handling I can generate an even more robust assay with lower chance of false positive. Z score and CV were calculated using the following equations [83;84].

$$Z' = 1 - \frac{3(\text{SD of high control} + \text{SD of low control})}{(\text{Average high control} - \text{Average low control})}$$

$$\%CV = \frac{100\ \text{SD of the test wells}}{\text{Average of the test wells}}$$

Using the automated assay I have performed a preliminary screen of five thousand compounds. There was at least 20 compounds produced more than 50% inhibition. Currently, I am evaluating the drug like property of these molecules using Lipinski rule. According to this rule, chemical properties such as molecular weight, solubility, polar surface area, number of rotatable bonds and number of H-bond donor and acceptor must be within a defined range for a molecule to become drug-like. Using this rule compounds will be shortlisted and re-tested for their inhibitor property in a 12-point dose-response experiment to confirm them as hits.

CHAPTER 6

CONCLUSION [5]

TSEs are dreadful diseases that produce a 100% fatality rate and a progressive and rapid deterioration which leads to complete disability. Currently, there is no therapy available against prion disorders [5]. The self-propagating protein misfolding process that features prion diseases amplifies the toxic and infectious prion in a logarithmic scale making it difficult for development of an efficient therapy at the symptomatic phase. Since there is still no test available to diagnose prion disease at the pre-symptomatic stage[85], the top priority is to develop strategies that could be beneficial after the patients show the first clinical signs of the disease.

Considering that a central event in TSEs is the conversion of PrP^{C} into PrP^{Sc}, a widely pursued therapeutic strategy has been to disrupt PrP^{Sc} formation. This approach has been extensively explored by many groups and some compounds have been identified with activity in vitro and in vivo. The list of compounds studied include: Polyanionic molecules, dextran sulphate, pentosan polysulphate, heparin sulphate mimetics, Phosphorothioate oligonucleotides, congo red analogs, suramin, curcumin, quinacrine,

[5]A significant portion of this chapter has been previously published in the following article. (Reproduced with permission, see appendix)

Mukherjee,A., Morales-Scheihing, D., Gonzalez-Romero,D., Green,K., Taglialatela,G., and Soto,C. (2010) Inhibition of Calcineurin Activation Increases Survival and Decreases Neurodegeneration at the Clinical Phase of Prion Disease. ***PLoS Pathogens*** 6(10) : e1001138

dendritic polyamines, tetracycline, amphotericin B, beta-sheet breaker peptides, anti-PrP antibodies, etc (for reviews, see [64;65;86]). However, these compounds produce a benefit mostly when they are administered during the pre-symptomatic stage of the disease, long before the appearance of clinical symptoms. Despite of the lack of positive results in animal models at the clinical phase of the disease, the unmet need for a medicine to treat patients resulted in human clinical trials with at least 3 of these drugs: quinacrine, amphotericin B and pentosan polysulphate [64]. Quinacrine, chlorpromazine, and some of their tricyclic derivatives were described as efficient inhibitors of PrP^{Sc} formation in murine neuroblastoma cells chronically infected with scrapie [87;88]. However, subsequent animal experiments failed to demonstrate efficacy in the treatment of TSEs, [89] even after intraventricular infusion [90]. Because quinacrine and chlorpromazine have been used in human medicine as anti-malarial and anti-psychotic drugs, respectively, they were tested in small clinical trials. No therapeutic effect was seen following quinacrine treatment in two independent trials, although some transient improvement occasionally occurred [91;92]. Amphothericin B and some of its analogues inhibited prion replication in infected cell cultures [93] and delayed the appearance of spongiosis, astrogliosis, and PrP^{Sc} accumulation in the brain of scrapie-infected hamsters [93;94]. However, an attempt to treat a CJD patient with amphothericin B was unsuccessful [95]. In view of its high systemic toxicity, these results decrease hopes that amphothericin B will prove useful in prion disease therapy. Several *in vitro* and *in vivo* studies have suggested pentosan polysulphate may be useful in prion diseases [90;96;97]. Pentosan polysulphate is marketed in some countries as a treatment for interstitial cystitis

and as anticoagulant, although its side effects include hemorrhage and hypersensitivity reactions. The main problem for using this drug for TSEs is that it does not cross the blood-brain barrier, so it has to be administered either early (during the peripheral prion replication phase) or directly into the brain. Several small observational trials by intra-cerebroventricular infusion of pentosan polysulphate have been conducted, some of them showing promising results [98-100]. However, the fact that the drug has to be administered directly into the brain makes its routine use very complicated.

My approach provides a novel molecular target down-stream of the prion misfolding process and aims to prevent the signaling pathways leading to synaptic alterations and neuronal death. My data suggests that the pathway by which PrP^{Sc} induces neurodegeneration involves ER-stress, alterations in calcium homeostasis and hyperactivation of CaN, a key brain phosphatase that controls important signaling events modulating neuronal fate and functioning [50]. These findings indicate that down regulation of CaN activity may be a promising target for prion disease therapy. Fortunately, there are known CaN inhibitors extensively studied, such as FK506 and Cyclosporin [39]. FK506 is an FDA approved drug that is used to prevent transplant regression [75]. The drug is sold under the name of Tacrolimus or Prograf. FK506 is produced by Streptomyces tsukubaensis [101]. By inhibiting CaN, the drug suppresses both humoral and cellular immune responses. As an FDA approved drug, the pharmacological properties of the compound are very well-known.

My results show that administration of FK506 during the symptomatic phase of the disease produced a significant delay of the disease progression manifested as an improvement on behavioral abnormalities and increase survival time compared to controls treated with vehicle. The effect is not dependent on the immunosuppressant activity of FK506, since rapamycin (a drug with similar immunosupressive effect, but not acting through CaN) did not produce any change on prion disease[102]. Moreover, administration of FK506 did not alter the pattern of brain inflammation, suggesting that the beneficial effect of this compound is not mediated by neuroimmune pathways. Treatment with FK506 led to a significant increase of pCREB and pBAD levels in the brain, which paralleled the decrease of CaN activity. Importantly, I observed lower degree of neurodegeneration in animals treated with the drug, which was revealed by a higher number of neurons and a lower quantity of degenerating nerve cells. These changes were not dependent on PrP^{Sc} formation, since the protein accumulated in the brain to the same levels as in the untreated mice.

Interestingly, it has been reported that neurodegeneration in other brain diseases associated to protein misfolding also involves ER-stress, changes on calcium homeostasis and CaN activation [63;103-105]. Recent studies have shown an increase in calcineurin signaling during the early clinical symptoms of Alzheimer's disease [106]. Strikingly, administration of FK506 to transgenic mice models of Alzheimer's disease restore memory deficits associated to the accumulation of amyloid-beta oligomers [107;108]and reduced long-term potentiation deficits produced by aggregated amyloid-beta. These

findings indicate that CaN may play a general role in neurodegenerative diseases and could serve as a novel target for therapeutic intervention in these devastating diseases.

To further develop the therapeutic strategy, based on optimization of CaN activity, I was awarded with NCDDN fellowship to develop a robust CaN activity assay compatible with high throughput screening of small molecules. I have performed a detailed characterization of the enzyme using a 96 well format and very carefully monitored the effect of different handling conditions. Finally I was able to convert an absorbance based phosphatase assay into a highly sensitive low volume fluorescence assay compatible with HTS. Interestingly I did produce high sensitivity without producing much dispersion of the data set. The assay was characterized by a Z score of 0.65 in a full plate done by hand. With automated liquid handling I was able to improve it even more up to 0.8, which is excellent for HTS assay.

Currently there is no treatment for prion disease. My work has identified and validated a novel therapeutic target against prion disorders. The highly sensitive and robust assay I developed will permit to identify novel compounds with the potential to treat prion disease and related neurodegenerative disorders.

APPENDIX

Copy Right Clearance from the Bentham Science Publishers Ltd

Grant of Permission:

Dear Dr. Mukherjee:

Thank you for your interest in our copyrighted material, and for requesting permission for its use. Permission is granted for the following subject to the conditions outlined below:

Endoplasmic Reticulum Stress Response in Prion Diseases pp.127-135 (9) Authors: Abhisek Mukherjee, Claudio Soto. Doi: 10.2174/978160805013010901010127

To be used in the following manner:

1. Bentham Science Publishers grants you the right to reproduce the material indicated above on a one-time, non-exclusive basis, solely for the purpose described. Permission must be requested separately for any future or additional use.
2. For an article, the copyright notice must be printed on the first page of article or book chapter. For figures, photographs, covers, or tables, the notice may appear with the material, in a footnote, or in the reference list.

Thank you for your patience while your request was being processed. If you wish to contact us further, please use the address below.

Sincerely,

AMBREEN IRSHAD

***Permissions & Rights* Manager**

Bentham Science Publishers Ltd

Email: permission@benthamscience.org

URL: www.benthamscience.com

Copy Right Clearance from the journal of Elesvier

Grant Permission:

ELSEVIER LICENSE TERMS AND CONDITIONS

Apr 04, 2012

This is a License Agreement between Abhisek Mukherjee ("You") and Elsevier ("Elsevier") provided by Copyright Clearance Center ("CCC"). The license consists of your order details, the terms and conditions provided by Elsevier, and the payment terms and conditions.

All payments must be made in full to CCC. For payment instructions, please see information listed at the bottom of this form.

Supplier	Elsevier Limited The Boulevard,Langford Lane Kidlington,Oxford,OX5 1GB,UK
Registered Company Number	1982084
Customer name	Abhisek Mukherjee
Customer address	7900 Cambridge St Houston, TX 77054
License number	2844841020643
License date	Feb 09, 2012
Licensed content publisher	Elsevier
Licensed content publication	Current Opinion in Cell Biology
Licensed content title	Role of calcineurin in neurodegeneration produced by misfolded proteins and endoplasmic reticulum stress
Licensed content author	Abhisek Mukherjee,Claudio Soto
Licensed content date	April 2011
Licensed content volume number	23
Licensed content issue number	2
Number of pages	8
Start Page	223
End Page	230
Type of Use	reuse in a thesis/dissertation
Portion	full article
Format	both print and electronic
Are you the author of this Elsevier article?	Yes

Copy Right Clearance from the journal of Plos Pathogens.

Hi Abhisek,

Actually, one of the most exciting things about PLoS and something central to its mission statement as a nonprofit company is the free and open access to the articles we publish. Bloggers, pop science writers, scientists, etc., can and do freely link and copy the articles published on our web site. The only legal obligation they have is to cite the original source. In the case of your paper, that would be you. When presenting your dissertation, you will need to cite you and your coauthors' authorship of your paper, something I imagine you were already planning on doing.

In case you are curious, our policy is explained in further detail here:
http://www.plospathogens.org/static/license.action
Don't hesitate to ask if you have any other questions.

Cheers,
Max

Max Vidrine
Publications Assistant
PLoS Pathogens
Public Library of Science
1160 Battery Street, Suite 100
San Francisco, CA 94111

GLOSSARY

AD	Alzheimer's Disease
ATP	Adenosine Triphosphate
BAD	Bcl_2 Associated death promoter
BDNF	Brain Derived Neuronal Growth Factor
Bmax	maximum activity
BSE	Bovine Spongiform Encephalopathy
Ca^{2+}	Bivalent calcium ion
CaM	Calmodulin
CaN	Calcineurin
Cn A	Calcineurin subunit A
Cn B	Calcineurin subunit B
Cn AI	Calcineurin autoinhibitory domain
CJD	Creutzfeldt - Jakob disease
CNS	Central Nervous System
CREB	cAMP Response Element Binding
Cu^{2+}	Bivalent copper ion
CyPrP	Cytosolic PrP
Da	Dalton
ER	Endoplasmic Reticulum
ERAD	ER Associated Degradation

FFI	Fatal Familial Insomnia
GFAP	Glial Fibrillary Acidic Protein
GPI	Glycosylphosphatidylinositol
GrP	Glucose Regulated Protein
GSS	Gerstmann Sträussler Syndrome
HC	Hydrophobic Chain
HD	Huntington's Disease
HTS	High Throughput Screening
IC	Intra Cerebral
IP	Intra Peritoneal
IP_3R	Inositol-1,3,5 triphosphate Receptor
Ki	Substrat inhibition constant
Km_a	Michaelis–Menten constant (Apparent)
L	Liter
M	Molar
MALDI	Matrix-assisted laser desorption/ionization
Mg^{2+}	Bivalent magnesium ion
Mn^{2+}	Bivalent manganese ion
n	nano
Neu N	Neuronal nuclear antigen
OR	Octa-peptide Repeat
PDI	Protein Disulfide Isomerase;

PERK	PKR like ER Kinase;
PD	Parkinson's Disease
PP	Protein Phosphatase
PrP	Prion Protein;
PrP^{C}	Cellular form of Prion Protein
PrP^{Sc}	Abnormally folded form of Prion Protein
pQC	Pre-emptive Quality Control
RML	Rocky Mountain Laboratory
RyR	Raynodine Receptor;
SERCA	Sarcoplasmic/ER Ca^{2+} ATPase
UPR	Unfolded Protein Response
s	Substrate
TSEs	Transmissible Spongiform Encephalopathies
trkB	tropomyosin related kinase B
v	initial velocity
vCJD	variant Creutzfeldt - Jakob disease
v_{max}	Maximum velocity

REFERENCES

1 Bruce ME, Will RG, Ironside JW, McConnell I, Drummond D, Suttie A, McCardle L, Chree A, Hope J, Birkett C, Cousens S, Fraser H, Bostock CJ: Transmissions to mice indicate that 'new variant' CJD is caused by the BSE agent. Nature 1997;389:498-501.

2 Johnson RT: Prion diseases. Lancet Neurol 2005;4:635-642.

3 Brown P: Iatrogenic Creutzfeldt-Jakob disease. Aust N Z J Med 1990;20:633-635.

4 Llewelyn CA, Hewitt PE, Knight RS, Amar K, Cousens S, Mackenzie J, Will RG: Possible transmission of variant Creutzfeldt-Jakob disease by blood transfusion. Lancet 2004;363:417-421.

5 Aguzzi A, Calella AM: Prions: protein aggregation and infectious diseases. Physiol Rev 2009;89:1105-1152.

6 Riek R, Hornemann S, Wider G, Glockshuber R, Wuthrich K: NMR characterization of the full-length recombinant murine prion protein, mPrP(23-231). FEBS Lett 1997;413:282-288.

7 Harris DA: Trafficking, turnover and membrane topology of PrP. Br Med Bull 2003;66:71-85.

8 Abid K, Soto C: The intriguing prion disorders. Cell Mol Life Sci 2006;63:2342-2351.

9 Riek R, Hornemann S, Wider G, Billeter M, Glockshuber R, Wuthrich K: NMR structure of the mouse prion protein domain PrP(121-321). Nature 1996;382:180-182.

10 Vey M, Pilkuhn S, Wille H, Nixon R, DeArmond SJ, Smart EJ, Anderson RG, Taraboulos A, Prusiner SB: Subcellular colocalization of the cellular and scrapie prion proteins in caveolae-like membranous domains. Proc Natl Acad Sci U S A 1996;93:14945-14949.

11 Ma J, Lindquist S: Wild-type PrP and a mutant associated with prion disease are subject to retrograde transport and proteasome degradation. Proc Natl Acad Sci U S A 2001;98:14955-14960.

12 Hetz C, Maundrell K, Soto C: Is loss of function of the prion protein the cause of prion disorders? Trends Mol Med 2003;9:237-243.

13 Lasmezas CI: Putative functions of PrP(C). Br Med Bull 2003;66:61-70.

14 Brown DR, Qin K, Herms JW, Madlung A, Manson J, Strome R, Fraser PE, Kruck T, von Bohlen A, Schulz-Schaeffer W, Giese A, Westaway D, Kretzschmar H: The cellular prion protein binds copper in vivo. Nature 1997;390:684-687.

15 Waggoner DJ, Drisaldi B, Bartnikas TB, Casareno RL, Prohaska JR, Gitlin JD, Harris DA: Brain copper content and cuproenzyme activity do not vary with prion protein expression level. J Biol Chem 2000;275:7455-7458.

16 Bounhar Y, Zhang Y, Goodyer CG, LeBlanc A: Prion protein protects human neurons against Bax-mediated apoptosis. J Biol Chem 2001;276:39145-39149.

17 Kuwahara C, Takeuchi AM, Nishimura T, Haraguchi K, Kubosaki A, Matsumoto Y, Saeki K, Matsumoto Y, Yokoyama T, Itohara S, Onodera T: Prions prevent neuronal cell-line death. Nature 1999;400:225-226.

18 Solforosi L, Criado JR, McGavern DB, Wirz S, Sanchez-Alavez M, Sugama S, DeGiorgio LA, Volpe BT, Wiseman E, Abalos G, Masliah E, Gilden D, Oldstone MB, Conti B, Williamson RA: Cross-Linking Cellular Prion Protein Triggers Neuronal Apoptosis in Vivo. Science 2004.

19 Klohn PC, Farmer M, Linehan JM, O'Malley C, Fernandez de MM, Taylor W, Farrow M, Khalili-Shirazi A, Brandner S, Collinge J: PrP antibodies do not trigger mouse hippocampal neuron apoptosis. Science 2012;335:52.

20 Bueler H, Aguzzi A, Sailer A, Greiner RA, Autenried P, Aguet M, Weissmann C: Mice devoid of PrP are resistant to scrapie. Cell 1993;73:1339-1347.

21 Moore RC, Lee IY, Silverman GL, Harrison PM, Strome R, Heinrich C, Karunaratne A, Pasternak SH, Chishti MA, Liang Y, Mastrangelo P, Wang K, Smit AF, Katamine S, Carlson GA, Cohen FE, Prusiner SB, Melton DW, Tremblay P, Hood LE, Westaway D: Ataxia in prion protein (PrP)-deficient mice is associated with upregulation of the novel PrP-like protein doppel. J Mol Biol 1999;292:797-817.

22 Rossi D, Cozzio A, Flechsig E, Klein MA, Rulicke T, Aguzzi A, Weissmann C: Onset of ataxia and Purkinje cell loss in PrP null mice inversely correlated with Dpl level in brain. EMBO J 2001;20:694-702.

23 Sakaguchi S, Katamine S, Nishida N, Moriuchi R, Shigematsu K, Sugimoto T, Nakatani A, Kataoka Y, Houtani T, Shirabe S, Okada H,

Hasegawa S, Miyamoto T, Noda T: Loss of cerebellar Purkinje cells in aged mice homozygous for a disrupted PrP gene. Nature 1996;380:528-531.

24 Prusiner SB: Prions. Proc Natl Acad Sci U S A 1998;95:13363-13383.

25 Horiuchi M, Priola SA, Chabry J, Caughey B: Interactions between heterologous forms of prion protein: binding, inhibition of conversion, and species barriers. Proc Natl Acad Sci U S A 2000;97:5836-5841.

26 Kaufman RJ: Orchestrating the unfolded protein response in health and disease. Journal of Clinical Investigation 2002;110:1389-1398.

27 Lindholm D, Wootz H, Korhonen L: ER stress and neurodegenerative diseases. Cell Death Differ 2006.

28 Ma J, Wollmann R, Lindquist S: Neurotoxicity and neurodegeneration when PrP accumulates in the cytosol. Science 2002;298:1781-1785.

29 Rane NS, Kang SW, Chakrabarti O, Feigenbaum L, Hegde RS: Reduced translocation of nascent prion protein during ER stress contributes to neurodegeneration. Dev Cell 2008;15:359-370.

30 Kang SW, Rane NS, Kim SJ, Garrison JL, Taunton J, Hegde RS: Substrate-specific translocational attenuation during ER stress defines a pre-emptive quality control pathway. Cell 2006;127:999-1013.

31 Hetz CA, Soto C: Stressing Out the ER: A Role of the Unfolded Protein Response in Prion-Related Disorders. Curr Mol Med 2006;6:37-43.

32 Pinton P, Giorgi C, Siviero R, Zecchini E, Rizzuto R: Calcium and apoptosis: ER-mitochondria Ca2+ transfer in the control of apoptosis. Oncogene 2008;27:6407-6418.

33 Zalk R, Lehnart SE, Marks AR: Modulation of the ryanodine receptor and intracellular calcium. Annu Rev Biochem 2007;76:367-385.

34 Torres M, Castillo K, Armisen R, Stutzin A, Soto C, Hetz C: Prion protein misfolding affects calcium homeostasis and sensitizes cells to endoplasmic reticulum stress. PLoS One 2010;5:e15658.

35 Jiang H, Xiong F, Kong S, Ogawa T, Kobayashi M, Liu JO: Distinct tissue and cellular distribution of two major isoforms of calcineurin. Mol Immunol 1997;34:663-669.

36 Cohen P, Cohen PT: Protein phosphatases come of age. J Biol Chem 1989;264:21435-21438.

37 Ingebritsen TS, Stewart AA, Cohen P: The protein phosphatases involved in cellular regulation. 6. Measurement of type-1 and type-2 protein phosphatases in extracts of mammalian tissues; an assessment of their physiological roles. Eur J Biochem 1983;132:297-307.

38 Cohen P: The structure and regulation of protein phosphatases. Annu Rev Biochem 1989;58:453-508.

39 Liu J, Farmer JD, Jr., Lane WS, Friedman J, Weissman I, Schreiber SL: Calcineurin is a common target of cyclophilin-cyclosporin A and FKBP-FK506 complexes. Cell 1991;66:807-815.

40 Lepre CA, Thomson JA, Moore JM: Solution structure of FK506 bound to FKBP-12. FEBS Lett 1992;302:89-96.

41 White DJ, Calne RY, Plumb A: Mode of action of cyclosporin A: a new immunosuppressive agent. Transplant Proc 1979;11:855-859.

42 Rusnak F, Mertz P: Calcineurin: form and function. Physiol Rev 2000;80:1483-1521.

43 Kissinger CR, Parge HE, Knighton DR, Lewis CT, Pelletier LA, Tempczyk A, Kalish VJ, Tucker KD, Showalter RE, Moomaw EW, .: Crystal structures of human calcineurin and the human FKBP12-FK506-calcineurin complex. Nature 1995;378:641-644.

44 Klee CB, Crouch TH, Krinks MH: Calcineurin: a calcium- and calmodulin-binding protein of the nervous system. Proc Natl Acad Sci U S A 1979;76:6270-6273.

45 Li HC: Activation of brain calcineurin phosphatase towards nonprotein phosphoesters by Ca2+, calmodulin, and Mg2+. J Biol Chem 1984;259:8801-8807.

46 Mukerjee N, McGinnis KM, Park YH, Gnegy ME, Wang KK: Caspase-mediated proteolytic activation of calcineurin in thapsigargin-mediated apoptosis in SH-SY5Y neuroblastoma cells. Arch Biochem Biophys 2000;379:337-343.

47 Wu HY, Tomizawa K, Matsui H: Calpain-calcineurin signaling in the pathogenesis of calcium-dependent disorder. Acta Med Okayama 2007;61:123-137.

48 Manalan AS, Klee CB: Activation of calcineurin by limited proteolysis. Proc Natl Acad Sci U S A 1983;80:4291-4295.

49 Liu F, Grundke-Iqbal I, Iqbal K, Oda Y, Tomizawa K, Gong CX: Truncation and activation of calcineurin A by calpain I in Alzheimer disease brain. J Biol Chem 2005;280:37755-37762.

50 Mansuy IM: Calcineurin in memory and bidirectional plasticity. Biochem Biophys Res Commun 2003;311:1195-1208.

51 Shibasaki F, Hallin U, Uchino H: Calcineurin as a multifunctional regulator. J Biochem 2002;131:1-15.

52 Hubbard MJ, Klee CB: Calmodulin binding by calcineurin. Ligand-induced renaturation of protein immobilized on nitrocellulose. J Biol Chem 1987;262:15062-15070.

53 Armstrong DL: Calcium channel regulation by calcineurin, a Ca2+-activated phosphatase in mammalian brain. Trends Neurosci 1989;12:117-122.

54 Burley JR, Sihra TS: A modulatory role for protein phosphatase 2B (calcineurin) in the regulation of Ca2+ entry. Eur J Neurosci 2000;12:2881-2891.

55 Lonze BE, Ginty DD: Function and regulation of CREB family transcription factors in the nervous system. Neuron 2002;35:605-623.

56 Shaywitz AJ, Greenberg ME: CREB: a stimulus-induced transcription factor activated by a diverse array of extracellular signals. Annu Rev Biochem 1999;68:821-861.

57 Tao X, Finkbeiner S, Arnold DB, Shaywitz AJ, Greenberg ME: Ca2+ influx regulates BDNF transcription by a CREB family transcription factor-dependent mechanism. Neuron 1998;20:709-726.

58 Huang EJ, Reichardt LF: Trk receptors: roles in neuronal signal transduction. Annu Rev Biochem 2003;72:609-642.

59 Bito H, Deisseroth K, Tsien RW: CREB phosphorylation and dephosphorylation: a Ca(2+)- and stimulus duration-dependent switch for hippocampal gene expression. Cell 1996;87:1203-1214.

60 Wang HG, Pathan N, Ethell IM, Krajewski S, Yamaguchi Y, Shibasaki F, McKeon F, Bobo T, Franke TF, Reed JC: Ca2+-induced apoptosis through calcineurin dephosphorylation of BAD. Science 1999;284:339-343.

61 Shou Y, Li L, Prabhakaran K, Borowitz JL, Isom GE: Calcineurin-mediated Bad translocation regulates cyanide-induced neuronal apoptosis. Biochem J 2004;379:805-813.

62 Agostinho P, Lopes JP, Velez Z, Oliveira CR: Overactivation of calcineurin induced by amyloid-beta and prion proteins. Neurochem Int 2008;52:1226-1233.

63 Reese LC, Zhang W, Dineley KT, Kayed R, Taglialatela G: Selective induction of calcineurin activity and signaling by oligomeric amyloid beta. Aging Cell 2008;7:824-835.

64 Weissmann C, Aguzzi A: Approaches to Therapy of Prion Diseases. Annu Rev Med 2005;56:321-344.

65 Trevitt CR, Collinge J: A systematic review of prion therapeutics in experimental models. Brain 2006;129:2241-2265.

66 Banks WA, Robinson SM, Diaz-Espinoza R, Urayama A, Soto C: Transport of prion protein across the blood-brain barrier. Exp Neurol 2009;218:162-167.

67 Hetz C, Russelakis-Carneiro M, Maundrell K, Castilla J, Soto C: Caspase-12 and endoplasmic reticulum stress mediate neurotoxicity of pathological prion protein. EMBO J 2003;22:5435-5445.

68 Kimberlin RH: Experimental scrapie in the mouse: a review of an important model disease. Sci Prog 1976;63:461-481.

69 Castilla J, Morales R, Saa P, Barria M, Gambetti P, Soto C: Cell-free propagation of prion strains. EMBO J 2008;27:2557-2566.

70 Castilla J, Saa P, Hetz C, Soto C: In vitro generation of infectious scrapie prions. Cell 2005;121:195-206.

71 Deininger MH, Weinschenk T, Meyermann R, Schluesener HJ: The allograft inflammatory factor-1 in Creutzfeldt-Jakob disease brains. Neuropathol Appl Neurobiol 2003;29:389-399.

72 Liu F, Schafer DP, McCullough LD: TTC, fluoro-Jade B and NeuN staining confirm evolving phases of infarction induced by middle cerebral artery occlusion. J Neurosci Methods 2009;179:1-8.

73 Mullen RJ, Buck CR, Smith AM: NeuN, a neuronal specific nuclear protein in vertebrates. Development 1992;116:201-211.

74 Rogers TB, Inesi G, Wade R, Lederer WJ: Use of thapsigargin to study Ca2+ homeostasis in cardiac cells. Biosci Rep 1995;15:341-349.

75 Scott LJ, McKeage K, Keam SJ, Plosker GL: Tacrolimus: a further update of its use in the management of organ transplantation. Drugs 2003;63:1247-1297.

76 Betmouni S, Clements J, Perry VH: Vacuolation in murine prion disease: an informative artifact. Curr Biol 1999;9:R677-R679.

77 Siskova Z, Page A, O'Connor V, Perry VH: Degenerating synaptic boutons in prion disease: microglia activation without synaptic stripping. Am J Pathol 2009;175:1610-1621.

78 Perry VH, Cunningham C, Boche D: Atypical inflammation in the central nervous system in prion disease. Curr Opin Neurol 2002;15:349-354.

79 Aramburu J, Heitman J, Crabtree GR: Calcineurin: a central controller of signalling in eukaryotes. EMBO Rep 2004;5:343-348.

80 Schmued LC, Hopkins KJ: Fluoro-Jade: novel fluorochromes for detecting toxicant-induced neuronal degeneration. Toxicol Pathol 2000;28:91-99.

81 Mondragon A, Griffith EC, Sun L, Xiong F, Armstrong C, Liu JO: Overexpression and purification of human calcineurin alpha from Escherichia coli and assessment of catalytic functions of residues surrounding the binuclear metal center. Biochemistry 1997;36:4934-4942.

82 Zuck P, O'Donnell GT, Cassaday J, Chase P, Hodder P, Strulovici B, Ferrer M: Miniaturization of absorbance assays using the fluorescent properties of white microplates. Anal Biochem 2005;342:254-259.

83 Cassaday J, Shah T, Murray J, O'Donnell GT, Kornienko O, Strulovici B, Ferrer M, Zuck P: Miniaturization and automation of an ubiquitin ligase cascade enzyme-linked immunosorbent assay in 1,536-well format. Assay Drug Dev Technol 2007;5:493-500.

84 Zuck P, O'Donnell GT, Cassaday J, Chase P, Hodder P, Strulovici B, Ferrer M: Miniaturization of absorbance assays using the fluorescent properties of white microplates. Anal Biochem 2005;342:254-259.

85 Soto C: Diagnosing prion diseases: needs, challenges and hopes. Nat Rev Microbiol 2004;2:809-819.

86 Sim VL, Caughey B: Recent advances in prion chemotherapeutics. Infect Disord Drug Targets 2009;9:81-91.

87 Doh-ura K, Iwaki T, Caughey B: Lysosomotropic agents and cysteine protease inhibitors inhibit scrapie-associated prion protein accumulation. J Virol 2000;74:4894-4897.

88 Korth C, May BC, Cohen FE, Prusiner SB: Acridine and phenothiazine derivatives as pharmacotherapeutics for prion disease. Proc Natl Acad Sci U S A 2001;98:9836-9841.

89 Barret A, Tagliavini F, Forloni G, Bate C, Salmona M, Colombo L, De LA, Limido L, Suardi S, Rossi G, Auvre F, Adjou KT, Sales N, Williams A, Lasmezas C, Deslys JP: Evaluation of quinacrine treatment for prion diseases. J Virol 2003;77:8462-8469.

90 Doh-ura K, Ishikawa K, Murakami-Kubo I, Sasaki K, Mohri S, Race R, Iwaki T: Treatment of transmissible spongiform encephalopathy by intraventricular drug infusion in animal models. J Virol 2004;78:4999-5006.

91 Nakajima M, Yamada T, Kusuhara T, Furukawa H, Takahashi M, Yamauchi A, Kataoka Y: Results of quinacrine administration to patients with Creutzfeldt-Jakob disease. Dement Geriatr Cogn Disord 2004;17:158-163.

92 Collinge J, Gorham M, Hudson F, Kennedy A, Keogh G, Pal S, Rossor M, Rudge P, Siddique D, Spyer M, Thomas D, Walker S, Webb T, Wroe S, Darbyshire J: Safety and efficacy of quinacrine in human prion disease (PRION-1 study): a patient-preference trial. Lancet Neurol 2009;8:334-344.

93 Mange A, Nishida N, Milhavet O, McMahon HE, Casanova D, Lehmann S: Amphotericin B inhibits the generation of the scrapie isoform of the prion protein in infected cultures. J Virol 2000;74:3135-3140.

94 Adjou KT, Privat N, Demart S, Deslys JP, Seman M, Hauw JJ, Dormont D: MS-8209, an amphotericin B analogue, delays the appearance of spongiosis, astrogliosis and PrPres accumulation in the brain of scrapie-infected hamsters. J Comp Pathol 2000;122:3-8.

95 Masullo C, Macchi G, Xi YG, Pocchiari M: Failure to ameliorate Creutzfeldt-Jakob disease with amphotericin B therapy. J Infect Dis 1992;165:784-785.

96 Caughey B, Raymond GJ: Sulfated polyanion inhibition of scrapie-associated PrP accumulation in cultured cells. J Virol 1993;67:643-650.

97 Diringer H, Ehlers B: Chemoprophylaxis of scrapie in mice. J Gen Virol 1991;72 (Pt 2):457-460.

98 Bone I, Belton L, Walker AS, Darbyshire J: Intraventricular pentosan polysulphate in human prion diseases: an observational study in the UK. Eur J Neurol 2008;15:458-464.

99 Terada T, Tsuboi Y, Obi T, Doh-ura K, Murayama S, Kitamoto T, Yamada T, Mizoguchi K: Less protease-resistant PrP in a patient with sporadic CJD treated with intraventricular pentosan polysulphate. Acta Neurol Scand 2010;121:127-130.

100 Tsuboi Y, Doh-ura K, Yamada T: Continuous intraventricular infusion of pentosan polysulfate: clinical trial against prion diseases. Neuropathology 2009;29:632-636.

101 Pritchard DI: Sourcing a chemical succession for cyclosporin from parasites and human pathogens. Drug Discov Today 2005;10:688-691.

102 Saunders RN, Metcalfe MS, Nicholson ML: Rapamycin in transplantation: a review of the evidence. Kidney Int 2001;59:3-16.

103 Matus S, Lisbona F, Torres M, Leon C, Thielen P, Hetz C: The stress rheostat: an interplay between the unfolded protein response (UPR) and autophagy in neurodegeneration. Curr Mol Med 2008;8:157-172.

104 Ghribi O: The role of the endoplasmic reticulum in the accumulation of beta-amyloid peptide in Alzheimer's disease. Curr Mol Med 2006;6:119-133.

105 Rao RV, Bredesen DE: Misfolded proteins, endoplasmic reticulum stress and neurodegeneration. Curr Opin Cell Biol 2004;16:653-662.

106 Abdul HM, Sama MA, Furman JL, Mathis DM, Beckett TL, Weidner AM, Patel ES, Baig I, Murphy MP, LeVine H, III, Kraner SD, Norris CM: Cognitive decline in Alzheimer's disease is associated with selective changes in calcineurin/NFAT signaling. J Neurosci 2009;29:12957-12969.

107 Dineley KT, Hogan D, Zhang WR, Taglialatela G: Acute inhibition of calcineurin restores associative learning and memory in Tg2576 APP transgenic mice. Neurobiol Learn Mem 2007;88:217-224.

108 Taglialatela G, Hogan D, Zhang WR, Dineley KT: Intermediate- and long-term recognition memory deficits in Tg2576 mice are reversed with acute calcineurin inhibition. Behav Brain Res 2009;200:95-99.

VITA

This dissertation was written by Abhisek Mukherjee. He was born on February19th, 1982 in Naihati, India. He finished his schooling from NNV and earned the highly competitive National Scholarship to join one of the most prestigious colleges in India, Presidency College Calcutta in 2000. Obtaining a Bachelors degree in Chemistry he was again selected for the National Scholarship to pursue a Master's degree in Biophysics and Molecular Biology in the University of Calcutta, India in 2003. In the year 2005 he obtained his masters degree with 33rd rank all over India in Graduate Aptitude Test of Engineering (GATE) for Biotechnology. In the mean time he was also awarded with Lt. Col. A.N. Bose scholarship from the University of Calcutta to continue higher education in the United States. On August 2005 Abhisek was accepted in the Graduate School of Biomedical Sciences in UTMB. In 2006 Abhisek decide to join the department of Biochemistry and Molecular Biology to conduct his dissertation research on the molecular basis of prion pathogenesis under the guidance of Dr. Claudio Soto. During his dissertation research he has authored five publications having potential effect in the field. One of them was cited in nature methods. He was also selected for several prestigious awards including Arthur V. Simmang Academic Scholarship, Michael Tacheeni Scott Endowed Scholarship and Young Investigator Scholarship from Alzheimer's Drug Discovery Foundation. Finally he was awarded with very prestigious and competitive NCDDN fellowship award which allowed him to spend one year in

Harvard Neuro Discovery Center (2010-2011) to learn high throughput screening of small molecule inhibitors that significantly contributed in his dissertation research.

List of Awards/Honors/Fellowships:

2011 : Arthur V. Simmang Academic Scholarship from Graduate School of Biomedical Sciences, University of Texas Medical Branch at Galveston.

2011 : Michael Tacheeni Scott Endowed Scholarship from Graduate School of Biomedical Sciences, University of Texas Medical Branch at Galveston.

2010 : Young Investigator Scholarship from Alzheimer's Drug Discovery Foundation.

2010 : Graduate Scholar Incentive Award from Graduate School of Biomedical Sciences, University of Texas Medical Branch at Galveston.

2009-2010: National Center for Drug Discovery in Neurodegeneration NIH/NINDS Cooperative Agreement Award (u24) for conducting research on assay development and high throughput screening of small molecule inhibitors in Harvard Neuro Discovery Center for a year.

2008 : Outstanding Leadership Award form Mitchell Center for Neurodegenerative Disorders, University of Texas Medical Branch at Galveston.

2005-2007: Selected for GATE (Graduate Aptitude Test in Engineering) Scholarship; Rank 34 all over India.

2005-2006: Lt. Col. A.N. Bose Award to pursue Higher Education in the USA from Univ. of Calcutta, Kolkata, India.

2003-2005: National Scholarship from Govt. of India for Academic Excellence.

Presentation/Abstracts:

1. Rodrigo Diaz, **Abhisek Mukherjee,** Claudio Soto. (2011) "Salty-Prion": A role of kosmotropic anions on PrP misfolding. ***Prion 2011.*** Montreal, Canada.

2. 4th Drug Discovery for Neurodegeneration Conference ***2010*** Houston, TX, USA.

3. Claudio Soto, Marcelo Barria, Baian Chen, Dennisse Gonzalez-Romero, **Abhisek Mukherjee**, Rodrigo Morales. (2009) Quantification of PrPSc in different blood fractions, brain and peripheral tissues at distinct stages of prion disease. ***Prion 2009.*** Sithonia, Greece.

4. Marcelo Barria, **Abhisek Mukherjee,** Dennisse Gonzalez-Romero, Rodrigo Morales, and Claudio Soto. (2008) De novo generation of infectious prions in vitro produces a new disease. ***Prion 2008.*** Spain, Madrid.

5. Claudio Soto, Marcelo Barria, Joaquin Castilla, Dennisse Gonzalez-Romero, **Abhisek Mukherjee,** Paula Saa and Rodrigo Morales. (2008) Generation of a constellation of new prions in vitro leading to the emergence of novel prion diseases. ***Prion 2008.*** Spain, Madrid.

6. **Abhisek Mukherjee,** Kristi Green, Dennisse Gonzalez-Romero, Giulio Taglialatela and Claudio Soto. (2008) Blocking calcineurin activity as a novel therapeutic approach for Prion disorders. ***Prion 2008.*** Spain, Madrid.

7. Claudio Soto, **Abhisek Mukherjee,** Rodrigo Morales, and Claudio Hetz. (***2007***) Mechanisms of Prion Neurotoxicity. ***Keystone Symposia: Apoptotic and Non-Apoptotic Cell Death Pathways (Z4).*** Monterey, California.

List of Publications:

A. ARTICLES IN PEER REVIEWED JOURNALS:

1.Diaz,C., **Mukherjee, A**., Soto,C. (2011) Kosmotropic Anions Promote Conversion of Recombinant Prion Protein into a PrPSc-like Misfolded Form. ***PLoS ONE***. *(*Manuscript under revision).

2.**Mukherjee,A.**, Soto,C. (2011) Role of Calcineurin in Neurodegeneration Produced by Misfolded Proteins and Endoplasmic Reticulum Stress. ***Current opinion in Cell Biology.*** 23(2):223-30. (**Impact Factor 14.153**)

3.**Mukherjee,A.,** Morales-Scheihing, D., Gonzalez-Romero,D., Green,K., Taglialatel,G., and Soto,C. (2010) Inhibition of Calcineurin Activation Increases Survival and Decreases Neurodegeneration at the Clinical Phase of Prion Disease. ***PLoS Pathogen*** 6(10) : e1001138. **(Impact Factor 8.978)**

4. Barria, M.A., **Mukherjee, A.,** Gonzalez-Romero, D., Morales, R. and Soto, C. (2009) De novo Generation of Infectious Prions in vitro Produces a New Disease Phenotype. ***PLoS Pathogen*** 5(5):e1000421. **(Impact Factor 8.978)** *

*This article has been highlighted in ***Nature Methods*** 6, 556 - 557 (2009).

B.BOOK CHAPTER:

5. **Mukherjee, A.,** Soto.C (2009) ER Stress Response in Prion Diseases. ***Bentham e Books.*** **eISBN:** 978-1-60805-013-0.